Cold atoms in the presence of disorder

Boris Shapiro
Department of Physics, Technion-Israel Institute of Technology,
Haifa 32000, Israel

December 30, 2011

Abstract

The review deals with the physics of cold atomic gases in the presence of disorder. The emphasis is on the theoretical developments, although several experiments are also briefly discussed. The review is intended to be pedagogical, explaining the basics and, for some of the topics, presenting rather detailed calculations .

1 Introduction

The behavior of cold atoms and Bose-Einstein condensates (BEC) in the presence of a random potential is an active area of research, and several reviews on the subject had already appeared [1, 2, 3, 4, 5, 6]. Those reviews discuss, among other things, the experimental work on BEC spreading in a disordered wave guide, which have culminated in the observation of one-dimensional Anderson localization [7, 8]. The present review is devoted to two and three dimensional systems of cold atoms, and it concentrates on topics not extensively covered in the previous reviews. There exists considerable amount of theoretical work on the subject, and recently few experimental results on spreading of an atomic cloud, in two [9] and three [10, 11] dimensions, have been published. The review is intended to be self contained and pedagogical, accessible to people without a solid background in the physics of disorder. It therefore contains a significant amount of background material.

Disorder is, of course, a very old theme in condensed matter physics, and a lot of knowledge was accumulated over the years. Some of this existing

knowledge can be directly transferred to the field of cold atoms, although there are also considerable differences between the two fields. For one thing, a random potential for atoms is usually created optically (an optical speckle) and it differs, in some respects, from the common models used in condensed matter theory. Furthermore, in disordered electronic systems one is usually interested in the nature of eigenstates at the Fermi level, because this determines whether a given system is a metal or an insulator. In contrast, a typical transport experiment with an atomic BEC involves an expansion of the atomic cloud (a "matter wave packet") in the presence of disorder. Such a packet contains a broad spectrum of components, some of which can propagate whereas the others get localized. Nonlinear effects also come into play, especially at an early stage of the expansion.

The equilibrium properties of a disordered BEC are also of interest, in particular the phenomenon of the insulator-superfluid transition. When the density of particles is low, they can at most form a fragmented condensate, i.e. small disconnected lakes, with no coherent coupling between them (an insulator). With an increase of the particle density these lakes overlap and, at some critical density, a single coherent condensate is formed (a superfluid).

It would hardly be possible to cover, in a single review, all aspects of the broad and rapidly progressing field of disordered cold atom systems. The choice of topics reflects, to some extent, personal preferences of the author, and every effort was made to cover those topics with some depth, clarity and precision. The emphasis is made on identifying the relevant parameters and on discussing limiting cases, when simple and clear physics emerges. Such simplified discussion might not be sufficient for quantitative interpretation of the existing experiments but, at least, it provides a good starting point for appreciating the richness and complexity of the underlying physics.

Sections 2 and 3 of this review contain background material on speckle potentials and on behavior of a quantum particle in a random potential. Section 4 deals with a disordered BEC in equilibrium and discusses the conditions for a disorder induced insulator-superfluid transition. Section 5 is devoted to the dynamical problem of cold atoms expanding in the presence of disorder. Both BEC and Fermi gas are treated. A dynamical problem of a different type is considered in Section 6. There a BEC with an initial phase modulation undergoes free expansion. In the course of the expansion large density fluctuations can develop, resulting in "matter wave caustics". Some concluding remarks are presented in Section 7.

2 Optical speckles: A random potential for atoms

An external potential (not necessarily random) for atoms can be created by lasers [12, 13]. The laser radiation polarizes an atom and changes its energy, e.g. the ground state energy, by an amount

$$V(\mathbf{r}) = \frac{1}{2}\alpha(\omega)I(\mathbf{r}), \tag{1}$$

where $I(\mathbf{r})$ is the radiation intensity at the position $\mathbf{r}$ of the atom and $\alpha(\omega)$ is the atomic polarizability. The latter depends on the radiation frequency ω and on the properties of the atom, in particular, on the detuning $\delta = \omega - \omega_R$, where ω_R is a resonance frequency of the relevant atomic transition. The case $\delta > 0$ (blue detuning) corresponds to a positive (with respect to the unperturbed atomic ground state) potential, while $\delta < 0$ (red detuning) corresponds to a negative potential. Thus, a random pattern of light intensity, referred to as speckle pattern, will serve as a random potential for atoms. Such speckle potentials are widely used in experiments with cold atoms [7, 9, 10, 11, 14, 15, 16, 17]. Although there exists a rather comprehensive book on optical speckles [18], it is worthwhile to review the subject here, paying attention also to the most recent work [19, 20, 21, 22].

2.1 Qualitative discussion

A schematic set up for making a speckle pattern is depicted in Fig.1.

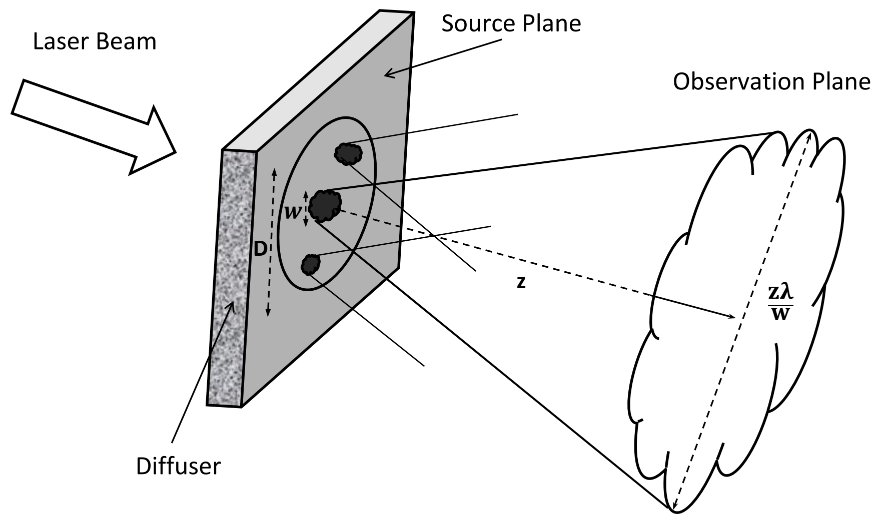

Figure 1: A laser beam, passing through a diffuser, illuminates an area of size D at the outgoing plane $z = 0$ (the source plane). Light from an elementary source of size w (three such sources are designated by black spots) propagates in a cone of angular width λ/w and illuminates a region of size $z\lambda/w$ in the observation plane. Waves emerging from different elementary sources interfere with each other, creating a speckle pattern.

A laser beam is transmitted through a diffuser. A common example of a diffuser is a glass plate with a rough surface (ground glass). Such a diffuser imprints a random phase on the transmitted radiation, while the intensity at the outgoing plane (the plane $z = 0$) simply follows the shape of the beam, e.g., a Gaussian laser beam. In the literature [18] one often studies a geometry when a plane wave (the central part of a laser beam) impinges on a circular or rectangular hole in a opaque screen, the hole being covered by a ground glass diffuser. In this case the light intensity is uniform within the corresponding circular or rectangular domain, and it is zero outside that domain. The

detailed geometry of the set up is not essential for the qualitative arguments.

Thus, an illuminated area, of size D, appears at the outgoing plane of the diffuser (the $z = 0$ plane, often referred to as source plane). This illuminated area can be viewed as a collection of sources, of a typical size w (usually, of the order of the radiation wavelength λ), with no spatial coherence between different sources. The sources are monochromatic, of frequency ω, and the $n'th$ source has a phase factor $e^{-i(\phi_n+\omega t)}$. Here n runs from 1 up to the total number of sources, $N_w \sim (D/w)^2$, and the phases ϕ_n change randomly from one source to another. The collection of such random sources at the $z = 0$ plane will produce a random, three-dimensional intensity pattern ("grains" of light) in the $z > 0$ half-space. By choosing some distant observation plane, $z = const$, one can study the transverse properties of such speckle patterns. Their longitudinal properties, such as the typical grain size in the z-direction, are also of interest. Although the detailed theory of speckles is rather intricate, a rough qualitative picture can be obtained by using a few basic facts about interference and diffraction.

We discuss the transverse properties first. An elementary source, of size w, in the source plane can be thought of as a particle of this size which scatters the incoming light or, alternatively, as a pinhole which diffracts the light. In either case the light will propagate in a cone of angular width $\sim \lambda/w$, illuminating a region of size $\sim z\lambda/w$ in the z-plane. Let's consider first the case $(z\lambda/w) > D$, i.e. $z > (Dw/\lambda) \equiv z^*$. This case corresponds to a "fully mixed" speckle, when all elementary sources contribute to the intensity at a typical point P in the z-plane. The electric field at some point P in the observation plane is a sum of many complex amplitudes, with random phases, originating from different areas at the source plane. As a result, the light intensity I across the observation plane is a random function of the position P, with the characteristic bright and dark spots. An estimate of the typical size of such speckle spot is analogous to the estimate of the separation between neighboring maxima and minima in the standard diffraction theory (the difference is that in the diffraction pattern from, say, a circular hole maxima and minima occur only in the radial direction, whereas in the speckle pattern they will be encountered in all directions). Let us denote by α_P the phase difference between the two waves arriving to the point P from the opposite edges of the illuminated area at the source plane. If the point P is moved by a distance $s_\perp$, the phase difference α_P will change by $\sim s_\perp D/\lambda z$, i.e., a shift of the observation point by a distance $s_\perp \sim \lambda z/D$ will change constructive interference to destructive. The distance $s_\perp$ provides an estimate

for the size of one speckle spot. Note that our discussion pertains to what is called "a free space geometry" [18], when the light propagates freely between the source plane and the observation plane. In practice one usually employs the "imaging geometry" [18], when a converging lens is placed between the two planes and the observation plane coincides with the focal plane of the lens. The speckle spot size then becomes $s_\perp \sim \lambda f/D$, where f is the focal length of the lens, and the minimal size is determined by the diffraction limit.

The picture outlined in the previous paragraph undergoes a profound change when the distance z to the observation plane becomes smaller than z^* - the so-called deep Fresnel zone [19, 20, 21, 22]. According to the above estimate, for $z \sim z^*$ a speckle spot reaches a size $s_\perp \sim w$. When z decreases further, a point P in the z-plane can receive radiation only from a limited number of the elementary sources, namely, the size of the region in the source plane which contributes to illumination of point P is $D_{eff} \sim \lambda z/w$. Using the above estimate for the speckle spot size, with D_{eff} instead of D, one obtains $s_\perp \sim \lambda z/D_{eff} \sim w$. Thus, $s_\perp \sim w$ holds starting from $z \sim z^*$ and all the way down to the minimal distance $z \sim w^2/\lambda$.

We now briefly discuss the structure of a speckle pattern in the longitudinal direction. Also in this direction the light intensity exhibits an irregular sequence of maxima and minima, and separation between those defines the typical size, $s_\parallel$, of the light "grain" in the z-direction. Standard diffraction theory [23] tells us that a significant change of intensity in the z-direction will occur when the corresponding phase, $D^2/\lambda z$, will change by amount of order unity, i.e. such a change will occur over a distance $s_\parallel \sim \lambda(z/D)^2$. In the deep Fresnel zone, $z < z^*$, one has to substitute D_{eff} for D, obtaining [21, 22] $s_\parallel \sim w^2/\lambda$.

2.2 Analytic treatment

Neglecting possible polarization effects, we consider a scalar field which can be thought of as one particular component of a monochromatic electric field. We denote the field at the source plane by $\psi(\boldsymbol{\rho}, 0)$, where the vector $\boldsymbol{\rho}$ designates the in-plane position and the second argument stands for $z = 0$. The function $\psi(\boldsymbol{\rho}, 0)$ is significant only within the region $|\boldsymbol{\rho}| \sim D$. The position in the observation plane z is denoted by $\mathbf{R}$. The field in this plane created

by the source field $\psi(\boldsymbol{\rho},0)$, is given by [24]:

$$\psi(\mathbf{R},z)=\int\frac{d^2q}{(2\pi)^2}\tilde{\psi}(\mathbf{q},0)\exp\left(i\mathbf{q}\cdot\boldsymbol{R}+i\sqrt{k_0^2-q^2}z\right), \tag{2}$$

where $k_0=\omega/c=2\pi/\lambda$, and

$$\tilde{\psi}(\mathbf{q},0)=\int d\boldsymbol{\rho}\psi(\boldsymbol{\rho},0)e^{-i\mathbf{q}\cdot\boldsymbol{\rho}}. \tag{3}$$

The expression (2) for $\psi(\mathbf{R},z)$ is exact, containing both propagating and evanescent waves, and it has a simple interpretation. For $z=0$ the source is Fourier expanded with respect to the transverse coordinate $\boldsymbol{\rho}$, and the factor $\exp(i\sqrt{k_0^2-q^2}z)$ is the "Fourier propagator" which relates the transverse Fourier transform at the z-plane, $\tilde{\psi}(\mathbf{q},\mathbf{z})$, to $\tilde{\psi}(\mathbf{q},\mathbf{0})$.

In the paraxial approximation the Fourier propagator is approximated by $\exp[ik_0z-(iq^2z/2k_0)]$. Substituting (3) into (2), with the approximated Fourier propagator, and performing integration over $\mathbf{q}$ leads to:

$$\psi(\mathbf{R},z)=\frac{k_0}{2\pi iz}e^{ik_0z}\int d\boldsymbol{\rho}\psi(\boldsymbol{\rho},0)\exp\left[i\frac{k_0}{2z}(\mathbf{R}-\boldsymbol{\rho})^{\mathbf{2}}\right], \tag{4}$$

which is the mapping of the source field, $\psi(\boldsymbol{\rho},0)$, onto the field $\psi(\mathbf{R},z)$ at the observation plane.

$\psi(\boldsymbol{\rho},0)$ is a random function of the position $\boldsymbol{\rho}$. It is described by the correlation function $\overline{\psi(\boldsymbol{\rho},0)\psi^*(\boldsymbol{\rho}',0)}$, where the overbar indicates a statistical average. Eq. (4) enables one to immediately write down the correlation function for the bulk speckle pattern, $\overline{\psi(\boldsymbol{R},z)\psi^*(\boldsymbol{R}',z')}$. We give the explicit expression only for the "transverse" correlation function ($z=z'$):

$$\overline{\psi(\boldsymbol{R},z)\psi^*(\boldsymbol{R}',z)}=\left(\frac{k_0}{2\pi z}\right)^2\int d\boldsymbol{\rho}d\boldsymbol{\rho}'\overline{\psi(\boldsymbol{\rho},0)\psi^*(\boldsymbol{\rho}',0)}\exp\left[i\frac{k_0}{z}(\triangle\boldsymbol{R}-\triangle\boldsymbol{\rho})\cdot(\boldsymbol{R}_0-\boldsymbol{\rho}_0)\right], \tag{5}$$

where $\triangle\boldsymbol{R}\equiv\boldsymbol{R}-\boldsymbol{R}'$, $\triangle\boldsymbol{\rho}\equiv\boldsymbol{\rho}-\boldsymbol{\rho}'$, and $\boldsymbol{R}_0\equiv\frac{1}{2}(\boldsymbol{R}+\boldsymbol{R}')$, $\boldsymbol{\rho}_0\equiv\frac{1}{2}(\boldsymbol{\rho}+\boldsymbol{\rho}')$.

This expression simplifies if one assumes a white noise source, i.e. $\overline{\psi(\boldsymbol{\rho},0)\psi^*(\boldsymbol{\rho}',0)}=\chi\overline{I}(\boldsymbol{\rho})\delta(\boldsymbol{\rho}-\boldsymbol{\rho}')$, where χ is a proportionality constant and $\overline{I}(\boldsymbol{\rho})=\overline{|\psi(\boldsymbol{\rho},0)|^2}$ is the average intensity at point $\boldsymbol{\rho}$ in the source plane. For this case one obtains [18]:

$$\overline{\psi(\boldsymbol{R},z)\psi^*(\boldsymbol{R}',z)}=\chi\left(\frac{k_0}{2\pi z}\right)^2\exp\left(i\frac{k_0}{z}\boldsymbol{R}_0\cdot\triangle\boldsymbol{R}\right)\int d\boldsymbol{\rho}\overline{I}(\boldsymbol{\rho})\exp\left(-i\frac{k_0}{z}\triangle\boldsymbol{R}\cdot\boldsymbol{\rho}\right), \tag{6}$$

which is proportional to the Fourier transform of $\overline{I}(\boldsymbol{\rho})$. If $\overline{I}(\boldsymbol{\rho})$ significantly differs from zero in a domain of size D, then the correlation function $\overline{\psi(\boldsymbol{R},z)\psi^*(\boldsymbol{R}',z)}$ decays on a characteristic scale $s_\perp \sim \lambda z/D$, which defines the typical transverse size of a speckle spot, as estimated in Sec. 2.1. For simple cases, when $\overline{I}(\boldsymbol{\rho})$ is constant within an aperture of a rectangular or circular shape, the integral in (6) can be evaluated explicitly [18]. Another simple and instructive example is $\overline{I}(\boldsymbol{\rho}) = I_0 \exp(-\rho^2/2D^2)$. The integral in (6) is then given by $2\pi D^2 \exp(-\frac{D^2 k_0^2 \triangle R^2}{2z^2})$ which, again, reveals the characteristic decay length $\lambda z/D$.

One can relax the assumption of a white noise source and consider a more general correlation function, at the source plane [21]:

$$\overline{\psi(\boldsymbol{\rho},0)\psi^*(\boldsymbol{\rho}',0)} = C(\triangle\boldsymbol{\rho})\overline{I}(\boldsymbol{\rho}_0), \tag{7}$$

where the function C decays on a shot scale, w, whereas the average intensity $\overline{I}$ changes on a much larger scale, D. Using this expression as an input in Eq. (5), one can derive the transverse properties of the speckle pattern. The term $k_0(\boldsymbol{\rho}\cdot\triangle\boldsymbol{\rho})/z \sim k_0 Dw/z$, in the exponent of Eq. (5), can be neglected for $z > Dw/\lambda \equiv z^*$. In this case the double integral in (5) factorizes into a product of two integrals which are the Fourier transforms of $I(\boldsymbol{\rho}_0)$ and $C(\triangle\boldsymbol{\rho})$. These Fourier transforms determine, respectively, the speckle spot size $s_\perp \sim \lambda z/D$ and the extent $\lambda z/w$ of the entire speckle pattern in the z-plane. In the opposite case, $z < z^*$, the speckle pattern "freezes", as described in Section 2.1.

The more general correlation function, $\overline{\psi(\boldsymbol{R},z)\psi^*(\boldsymbol{R}',z')}$, with $z \neq z'$, has been studied in detail in [21, 22], where the normalized function, $\gamma(\boldsymbol{R},z;\boldsymbol{R}',z') \equiv \overline{\psi(\boldsymbol{R},z)\psi^*(\boldsymbol{R}',z')}/\sqrt{\overline{I}(\boldsymbol{R},z)\overline{I}(\boldsymbol{R}',z')}$ was introduced (this function is denoted there by μ). Simple analytic expressions for $|\gamma(\boldsymbol{R},z;\boldsymbol{R}+\triangle\boldsymbol{R},z+\triangle z)|^2$ can be obtained if one chooses in (7) $C(\triangle\boldsymbol{\rho}) = \exp[-(\triangle\boldsymbol{\rho}/w)^2]$ and $\overline{I}(\boldsymbol{\rho}_0) = I_0 \exp[-(\boldsymbol{\rho}_0/D)^2]$ [21, 22]. In certain limiting cases the expression

$$|\gamma(\boldsymbol{R},z;\boldsymbol{R}+\triangle\boldsymbol{R},z+\triangle z)|^2 = \frac{1}{1+(\triangle z/s_\parallel)^2}\exp\left[-\frac{2(\triangle\boldsymbol{R}/s_\perp)^2}{1+(\triangle z/s_\parallel)^2}\right] \tag{8}$$

emerges. In the deep Fresnel zone $s_\parallel = \pi w^2/\lambda$ and $s_\perp = w$ (Eq. (12) in [22]), whereas in the Fresnel zone (and for $\triangle z$ not too large) $s_\parallel = \lambda z^2/\pi D^2$ and $s_\perp = \lambda z/\pi D$ [25]. The correlation function (8) is quite unusual: not only is it strongly anisotropic but also the effective correlation length in the transverse

direction, $s_{\perp eff} \sim s_\perp \sqrt{1 + (\triangle z / s_\parallel)^2}$, depends on the separation $\triangle z$ between the points in the longitudinal direction. Moreover, $s_{\perp eff}$ increases with $\triangle z$, so that long range correlations in the transverse direction develop.

A simpler three-dimensional potential, corresponding to the interference pattern in an ergodic cavity, was considered in [26]. It is fully isotropic and the square of the correlation function is

$$\gamma^2(\boldsymbol{r}) = sinc^2(2\pi r/\lambda), \tag{9}$$

where λ is the light wave length.

Let us recall that the potential acting on the atoms is proportional not to the field but to its intensity, see Eq.(1). Therefore, denoting $(\boldsymbol{R}, z) \equiv \boldsymbol{r}$, the correlation function for the potential, $\overline{V(\boldsymbol{r})V(\boldsymbol{r}')}$, is proportional to $\overline{I(\boldsymbol{r})I(\boldsymbol{r}')} = \overline{\psi(\boldsymbol{r})\psi^*(\boldsymbol{r})\psi(\boldsymbol{r}')\psi^*(\boldsymbol{r}')}$, which requires averaging of a product of four fields. For a Gaussian random function the latter reduces to the sum of two possible contractions of the fields, with the result [18]:

$$\overline{I(\boldsymbol{r})I(\boldsymbol{r}')} = \overline{I}(\boldsymbol{r})\overline{I}(\boldsymbol{r}') + |\overline{\psi(\boldsymbol{r})\psi^*(\boldsymbol{r}')}|^2. \tag{10}$$

Since $\overline{I}(\boldsymbol{r})$ changes on a scale much larger than the decay length of the correlation function, one can set $\overline{I}(\boldsymbol{r}) = \overline{I}(\boldsymbol{r}') \equiv I_0$. Rewriting (10) in terms of the potential then yields [26, 27]:

$$\overline{V(\boldsymbol{r})V(\boldsymbol{r}')} = V_0^2[1 + |\gamma(\boldsymbol{r} - \boldsymbol{r}')|^2], \tag{11}$$

where V_0 is the average value of the potential at point $\boldsymbol{r}$ and $\gamma = \overline{\psi(\boldsymbol{r})\psi^*(\boldsymbol{r}')}/I_0$ is the normalized correlation function of the speckle field. It follows from (11) that the second moment $\overline{V^2} = 2V_0^2$. The $n'th$ moment, $\overline{V^n}$, will involve averaging of n pairs of fields and thus $n!$ contractions, giving $\overline{V^n} = n!V_0^n$. This implies that the probability distribution of the potential value, at some point $\boldsymbol{r}$, is given by the Rayleigh distribution

$$P(V) = \frac{1}{V_0}\exp(-V/V_0), \tag{12}$$

where a blue detuned potential has been assumed (for red detuning both V and V_0 are negative, so that (12) should be written with a minus sign). The Rayleigh distribution for the intensity is a direct consequence of the fact that the speckle field - being a sum of many contributions with random phases - obeys the central limit theorem, i.e., the real and the imaginary part of the

field are Gaussian distributed [18]. The distribution $P(V)$ is not symmetric with respect to its average value V_0, and it is convenient to introduce the deviation $\delta V = V - V_0$, with the correlation function

$$\overline{\delta V(\boldsymbol{r})\delta V(\boldsymbol{r}')} = V_0^2 \Gamma\left(\frac{\boldsymbol{r}-\boldsymbol{r}'}{R_0}\right), \tag{13}$$

where $|\gamma|^2$ was denoted by Γ and the argument $(\boldsymbol{r}-\boldsymbol{r}')$ was rescaled by the correlation decay length R_0. Computer generated images of a speckle potential (in $2d$) can be found, e. g., in [26, 28].

Finally, let us mention that making an optical speckle is not the only way to create a random potential for atoms. Another option is to introduce into the system some foreign, "impurity" atoms, trapped in a random fashion at the nodes of an optical lattice [29]. These impurity atoms form a frozen, random pattern which scatters the mobile atoms of the system under investigation. This method for creating a random potential has been implemented in the recent study of a one-dimensional Bose system [30].

3 Quantum particle in a random potential

The behavior of a quantum particle in a random potential has been extensively studied in condensed matter physics [31, 32, 33, 34, 35, 36, 37]. The theoretical tools range from diagrammatic technique [35], to self-consistent approach [38], to field theory methods [36, 37]. The most popular model is that of a Gaussian random potential, with or without correlations (the latter case is known as the "white-noise limit"). This model features not only in condensed matter physics but also in the field of cold atoms, for instance, in the study of the disorder induced superfluid-insulator transition [39, 40]. The Gaussian potential differs in some respects from a speckle potential. The latter is bounded from below (blue detuning) or from above (red detuning). This will clearly lead to large changes in the particle behavior close to the boundary of the spectrum. In addition, the speckle potentials lack symmetry (in statistical sense, of course), with respect to the average value, so that products of an odd number of δV's do not average to zero. Therefore the diagram technique for a speckle potential [26, 27] differs somewhat from the standard one [35]. To a large extent, however, there are no qualitative differences, as long as one is in the weak scattering regime. In particular, the mean free path, calculated in the Born approximation, is "universal", in the

sense that it only depends on the correlation function (13) but not on the detailed statistics of the potential.

Consider a random potential $V(\boldsymbol{r})$, with some average value $\overline{V}$. This value is included into the unperturbed Hamiltonian, and the perturbation is $\delta V(\boldsymbol{r})$. Thus, the bottom of the unperturbed spectrum is $\overline{V}$ and, if the particle energy ϵ is reckoned from this point, the unperturbed spectrum is simply $\epsilon = \hbar^2 k^2/2m$. With this caveat, most of the ensuing discussion applies to a broad class of potentials, including speckle and Gaussian potentials. Viewing the potential relief from the "$\overline{V}$-level", one can envisage a collection of potentials barriers and wells, of typical magnitude V_0 and typical size R_0. It is convenient to define the "correlation energy"

$$E_0 = \frac{\hbar^2}{2mR_0^2}, \tag{14}$$

where m is the particle's mass. E_0 has the clear meaning of a zero point energy for a particle confined to a spatial region of size R_0. There are, thus, three relevant energy scales in our problem - the typical variation V_0 of the random potential, the correlation energy E_0 and the particle energy ϵ - and the physics depends on the two ratios: V_0/E_0 and $\epsilon/E_0 = (kR_0)^2$. In particular, $kR_0 << 1$ corresponds to short range correlations, when the correlation length R_0 is shorter than the de Broglie wavelength of the particle. The opposite case, $kR_0 >> 1$, describes smooth (on the wavelength scale) disorder, for which a semiclassical approximation might be a good starting point. The space dimension, d, is also an important factor. For $d = 1, 2$ all eigenstates (in an infinite system) are localized, while for $d = 3$ there is a critical energy E_c which separates between extended and localized states. In this review we concentrate on two and three dimensions.

The value of the parameter $(V_0/E_0) \equiv \eta$ is crucial for understanding the transport picture. For $\eta << 1$ a typical well is too weak to bind a particle. In this regime semiclassical considerations are not appropriate and classical percolation is of no relevance whatsoever for understanding the quantum localization transition. In the opposite case, $\eta >> 1$, there is a broad region in the particle energy spectrum, where semiclassical considerations do apply. The ultimate transition to localization is, of course, of quantum nature also for this case but now the transition occurs close (somewhat above) to the classical percolation threshold and an interesting crossover between classical percolation and Anderson localization takes place. All this is discussed below

in some detail. Before making various estimates and calculations, it is essential to specify whether η is large or small, and it is convenient to separately discuss the following cases:

3.1 $d = 3$ and $\eta << 1$

A particle of sufficiently high energy will be weakly scattered by the random potential and will propagate by diffusion. When the energy of the particle is lowered, the scattering becomes stronger and quantum interference effects cease to be negligible. These effects lead to Anderson localization [41] below some energy E_c, called the mobility edge.

Before trying to estimate E_c let us make the following remark: The $3d$ speckle potential is not "generic" in the sense that the integral $\int \Gamma(\mathbf{r}) d^3 r$ diverges, due to the long-range character of the correlation function $\Gamma(\mathbf{r})$ (see equations (8) and (9)). In contrast, the impurity potential, mentioned at the end of Sec. 2.2, belongs to the standard type of a "generic" potential, usually encountered in condensed matter physics. The expression for the mean free path, and therefore an estimate for E_c, depends on whether the potential is "generic" or not. In the forthcoming discussion the "generic" case will be considered first and, then, some necessary changes for the speckle potential will be pointed out.

Let us now estimate the characteristic energy near which the diffusive transport breaks down. Qualitatively, the random potential can be viewed as a collection of scatterers, of strength V_0 and size R_0. Since $V_0 << E_0$, a single scatterer can be treated within the Born approximation, regardless of the particle energy. One should, however, distinguish between "slow" particles, with energies $\epsilon << E_0$ (i.e. $kR_0 << 1$) and "fast" particles, satisfying $\epsilon >> E_0$ (i.e. $kR_0 >> 1$). For slow particles the scattering cross-section is estimated as [42] $\sigma \sim \eta^2 R_0^2$. Since the number of scatterers per unit volume is $n_{scat} \sim R_0^{-3}$, the mean free path

$$l = \frac{1}{\sigma n_{scat}} \sim \frac{1}{\eta^2} R_0 \sim \left(\frac{\hbar^2}{m}\right)^2 \frac{1}{V_0^2 R_0^3}. \qquad (15)$$

When one refers to "a quantum particle", one actually has in mind a wave packet with a well defined wave vector $\mathbf{k}$, such that the uncertainty $\triangle k \lesssim k$. The minimal size of such a packet is of the order of k^{-1} and, for the above reasoning to be consistent, this must be much smaller than l, which leads to

the requirement $kl >> 1$. The condition $kl \sim 1$ (the Ioffe-Regel criterion) corresponds to a characteristic energy

$$W \sim V_0 \eta^3 \sim \left(\frac{m}{\hbar^2}\right)^3 \left(V_0^2 R_0^3\right)^2 . \tag{16}$$

Thus, when the particle energy ϵ (counted from the average value of the potential) decreases and approaches W, the diffusive transport breaks down and quantum interference effects come into play in an essential way . The potential strength and range appear in Eqs. (15,16) only in the combination $V_0^2 R_0^3$.

We now return to the fast particles, with $\epsilon >> E_0$. Such high energy particles scatter primarily in the forward direction, within a cone of an angular width $\triangle\theta < 1/kR_0$. Therefore the scattering cross section for fast particles is $\sigma \sim \eta^2/k^2$ [42] (smaller by a factor $(1/kR_0)^2$ than the cross section for slow particles). Furthermore, the cross section relevant for transport is not σ but the transport cross section, $\sigma^* \sim \sigma/(kR_0)^2$. The small extra factor, $(1/kR_0)^2$, accounts for the fact that in a single scattering event the particle direction changes only by a small angle, randomly distributed in a cone of angular width $\Delta\theta \sim 1/kR_0$. Therefore it will take $(kR_0)^2$ scattering events to completely randomize the initial direction. Thus, the transport mean free path is:

$$l^* = \frac{R_0^3}{\sigma^*} \sim R_0 \left(\frac{\epsilon}{V_0}\right)^2 . \tag{17}$$

The qualitative estimate in Eqs. (15), (17) can be supported by a calculation based on a diagrammatic perturbation theory [35]. In that theory the transport mean free time τ^* is related to the correlation function of the potential. In the leading order in V_0^2, the inverse mean free time (the scattering rate) is expressed in terms of the Fourier transform $\tilde{\Gamma}(\mathbf{q})$ of the correlation function $\Gamma(\frac{\boldsymbol{R}}{R_0})$, defined in Eq. (13):

$$\begin{aligned}\frac{1}{\tau^*} &= \frac{2\pi}{\hbar} V_0^2 \int \frac{d^3k'}{(2\pi)^3} \tilde{\Gamma}(\mathbf{k}-\mathbf{k}') \delta\left(\epsilon - \frac{\hbar^2 k'^2}{2m}\right)(1-\cos\theta) \\ &= \frac{\pi}{\hbar} V_0^2 \nu \int_0^\pi d\theta \sin\theta \tilde{\Gamma}\left(2k\sin\frac{\theta}{2}\right)(1-\cos\theta),\end{aligned} \tag{18}$$

where $\epsilon = \frac{\hbar^2 k^2}{2m}$ is the particle energy and $\nu = mk/2\pi^2\hbar^2$ is the density of states (per spin) at that energy. The argument $2k\sin\frac{\theta}{2}$ corresponds to

the momentum transfer for (elastic) scattering at an angle θ and the factor $(1-\cos\theta)$ accounts for the difference between the scattering and the transport cross sections. Taking, for example, a Gaussian correlation function, $\Gamma = \exp(-R^2/R_0^2)$, performing the integral and writing the result in terms of $l^* = v\tau^*$ ($v = \hbar k/m$ is the particle velocity), yields

$$l^* = \frac{2R_0}{\sqrt{\pi}} \left(\frac{\epsilon}{V_0}\right)^2 \frac{1}{1-(1+k^2R_0^2)\exp(-k^2R_0^2)}. \tag{19}$$

For $kR_0 << 1$ one can expand the exponent, obtaining $l^* = 4R_0/\eta^2\sqrt{\pi}$ (compare to the qualitative estimate in (15)), whereas in the opposite case the result is simply $l^* = \frac{2R_0}{\sqrt{\pi}}(\frac{\epsilon}{V_0})^2$ (compare with (17)). Eq.(19) can be rewritten in terms of the diffusion coefficient $D_\epsilon = vl^*/3$. For the limiting cases the result is:

$$D_\epsilon = \begin{cases} \frac{\hbar}{m}\frac{4}{3\sqrt{\pi}}\left(\frac{\epsilon-\overline{V}}{W}\right)^{1/2} & , \quad W << (\epsilon-\overline{V}) << E_0 \\ (\frac{8V_0R_0^2}{\pi m})^{1/2}\left(\frac{\epsilon-\overline{V}}{V_0}\right)^{5/2} & , \quad \epsilon >> E_0 \end{cases} \tag{20}$$

Note that we have restored $\overline{V}$ in these expressions, to give them the more convenient form, "invariant" with respect to the choice of the reference energy. Other types of the correlation function $\Gamma(\mathbf{R})$ can be considered in a similar way. The order-of magnitude estimates (15), (17) do not depend on the specific shape of the correlation function, provided that $\int \Gamma(\mathbf{R})d^3R$ is finite.

Thus, for the case $\eta << 1$ the Born approximation is valid in a broad range of energies, the only condition being $(\epsilon - \overline{V}) >> W$. When $(\epsilon - \overline{V})$ approaches W, the Born approximation breaks down and the diffusion coefficient becomes of the order of $\hbar/m$. This is the natural unit of "quantum diffusion" (analogous to the quantum conductance $e^2/\hbar$) and it signals a crossover to a purely quantum mode of transport. At E_c the diffusion coefficient drops to zero. Somewhat above E_c it obeys a power law, $D_\epsilon \propto (\epsilon - E_c)^\nu$, with $\nu \approx 1.57$ [43]. Below E_c all states are localized. The exact position of E_c depends on the type of the random potential. It should be located somewhere in the vicinity of the average potential value $\overline{V}$, although the precise location, and even the sign (with respect to $\overline{V}$), is not known. The aforementioned Ioffe-Regel criterion marks breakdown of the diffusive transport but it does not enable one to determine the location of E_c. In technical terms, the

mean free path is related to the imaginary part of the self-energy, whereas E_c can be affected also by the real part, which causes a shift of the spectrum. The real part, calculated in the self-consistent Born approximation (see [44], [45] and Sec. 5.3), turns out to be negative, of the order of ηV_0, which indicates that E_c is below $\overline{V}$. One should keep in mind, however, that the self-consistent Born approximation is not really a controlled one.

For energies well below E_c, when $(E_c - \epsilon) >> W$, one enters the region of strongly localized states- the "Lifshitz tail". While for high energies the density of states $\nu(\epsilon)$ is close to that of a free particle, in the Lifshitz tail $\nu(\epsilon)$ is small and it depends on the type of the potential. For a Gaussian potential the tail was studied long ago, by the method of optimal fluctuation [46, 47, 32]. At extremely low energies, $(E_c - \epsilon) > E_0$, the optimal fluctuation is just a single well, of size R_0 and depth $\sim |\epsilon|$, which immediately leads to $\ln \nu(\epsilon) \propto -\epsilon^2/V_0^2$. For energies $W << E_c - \epsilon << E_0$ the optimal fluctuation is of different nature. In this energy interval a single well of size R_0 and depth $\sim |\epsilon|$ cannot bind a particle, and the optimal fluctuation corresponds to a much broader well, of radius $R_\epsilon \sim (\hbar^2/m|\epsilon|)^{1/2} >> R_0$. Since such a well is comprised of $\sim (R_\epsilon/R_0)^d$ "elementary" wells, the corresponding probability is $\exp(-\epsilon^2/V_0^2)$, raised to power $(R_\epsilon/R_0)^d$. This yields

$$\ln \nu(\epsilon) \propto -\left(\frac{\epsilon^2}{V_0^2}\right)\left(\frac{\hbar^2}{m|\epsilon|R_0^2}\right)^{d/2} \sim -\left(\frac{|\epsilon|}{E_t}\right)^{2-(d/2)} \quad , \quad E_t = \left(\frac{V_0^4}{E_0^d}\right)^{1/(4-d)} . \tag{21}$$

In $3d$, $E_t = W$, and in $2d$ it is the characteristic crossover energy V_0^2/E_0, which will be identified in Sec. 3.3. It is interesting to note that the same energy scale W (in $3d$) emerges both from the Ioffe-Regel criterion and from the analysis of the Lifshitz tail. The factor $\sim (R_\epsilon/R_0)^d$, entering the derivation of (21), can be also interpreted in a different way: Since the spatial extent of the localized wave function, R_ϵ, strongly exceeds the typical variation length R_0 of the random potential, the particle experiences not the original potential but an effective Gaussian potential with a variance smaller by a factor $(R_\epsilon/R_0)^d$.

In $3d$, (21) can be written as $\ln \nu(\epsilon) \sim -\mathcal{L}/R_\epsilon$, where $\mathcal{L} \sim R_0/\eta^2$ is a characteristic length, specifying the short range disorder, and termed the Larkin length in [40] (it is of the same order of magnitude as the mean free path in the weak scattering regime, (15)). The localized states in the Lifshitz tail are rare, separated by exponentially large distances, and the tunneling

amplitude between a pair of such states is exponentially small. When ϵ approaches the mobility edge, by a few E_t, the size of the localized wave function approaches $\mathcal{L}$, the overlap becomes significant and the tunneling amplitude is of the order of unity: the concept of the optimal fluctuation ceases to be relevant,

So far there have been no quantitative studies of the Lifshitz tails for speckle potentials in $2d$ and $3d$ (the $1d$ case was considered in [48]). For a red-detuned potential, which is not bounded from below, one can argue that Eq. (21) for the Lifshitz tail is still valid. Although the original potential is not Gaussian (see (12)), the particle localized in a optimal fluctuation feels an effective potential, obtained by integrating the original, "microscopic" potential over a volume R_ϵ^d. This results in an effective potential with an approximately Gaussian statistics, with a variance by the factor $(R_\epsilon/R_0)^d$ smaller than that of the original potential, so that (21) is recovered. This consideration does not hold in the extreme tail, $|\epsilon| < E_0$, when the optimal fluctuation is just a single well of depth $\sim |\epsilon|$ and size $\sim R_0$. The density of states then follows the tail of the potential distribution (12), i.e. $\ln \nu(\epsilon) \propto -|\epsilon|/V_0$.

For the blue-detuned speckle potential the picture is different. Here one can expect the validity of Eq. (21) only if the particle energy satisfies $W << (E_c - \epsilon) << V_0$, i.e. when ϵ is well below E_c but still far away from the bottom of the spectrum. When ϵ approaches the bottom of the spectrum, $\epsilon = 0$ (here it is natural to reckon the energy from the bottom of the spectrum), a new tail, of different nature emerges. Close to $\epsilon = 0$ the density of states can be estimated as follows [32] (the argument applies in any dimension d). In order to arrange for a state with a small energy, one has to "clean out" a region of size $R_\epsilon \sim (\hbar^2/m\epsilon)$, i.e. no barriers of height larger than ϵ should be allowed in that region. Such a region consists of many, $\sim (R_\epsilon/R_0)^d$, independent elements, of size R_0 each. The probability that the potential in a given element does not exceed ϵ is $\sim \epsilon/V_0$. Therefore, for $\epsilon \to 0$

$$\nu(\epsilon) \propto \left(\frac{\epsilon}{V_0}\right)^{(R_\epsilon/R_0)^d} \quad \Rrightarrow \quad \ln \nu(\epsilon) \propto -\left(\frac{E_0}{\epsilon}\right)^{d/2} ln\frac{V_0}{\epsilon} \tag{22}$$

The two expressions, (21) and (22) should match somewhere half way between the bottom of the spectrum and E_c.

As has been stated in the beginning of this section, for the 3d speckle potential the integral $\int \Gamma(\mathbf{r}) d^3 r$ diverges, so that the expression (15) for the

mean free path and the subsequent estimate for W do not apply. The formula (18), however, does apply and, for the ergodic cavity potential (9), it yields for the mean free path (in the small k limit, when there is no difference between l and l^*) [26]:

$$l = \left(\frac{\hbar^2}{m}\right)^2 \frac{k}{\pi V_0^2 R_0^2}, \tag{23}$$

with $R_0 = \lambda/2\pi$. Thus, for $kR_0 << 1$, the mean free path is proportional to k, unlike the k-independent result in (15). The condition $kl \sim 1$ will now give a characteristic energy V_0^2/E_0, instead of (16). This energy provides an estimate for E_c, with respect to $\overline{V}$.

Finally, the study of transport in a $3d$ anisotropic speckle potential, with correlation function (8) (or, possibly, even some more general and complicated cases [21, 22]) only begins and the first work on the subject has just appeared [49]. Due to the anisotropy, diffusion is described by a tensor which, in the weak scattering regime, can be computed with the help of the Fourier transform of (8):

$$\tilde{\Gamma}(\mathbf{q}_\perp, q_\parallel) = \pi\sqrt{2\pi}\, \frac{s_\perp s_\parallel}{q_\perp} \exp\left[-\frac{q_\perp^2 s_\perp^2}{8} - 2\left(\frac{q_\parallel s_\parallel}{q_\perp s_\perp}\right)^2\right] , \tag{24}$$

where $\mathbf{q}_\perp$ and $q_\parallel$ are the transverse and the longitudinal (i.e. z) component of the transmitted momentum. Because of the long range transverse correlations in the speckle potential (see the discussion after Eq. (8)) $\tilde{\Gamma}(\mathbf{q}_\perp, q_\parallel)$ has a peculiar essential singularity at $q_\perp = 0$. More theoretical work is needed in order to understand how such strongly anisotropic, "non-generic" potentials affect the standard picture of Anderson localization. It is worthwhile to note, however, that the subtle long-range correlations, of the kind given in (8), although important in principle, might be not so prominent in practice. For instance, according to the authors of [10], their speckle potential is well described by a (anisotropic) Gaussian correlation function which is, by definition, "generic" and short-ranged.

3.2 $d = 3$ and $\eta >> 1$

This is the case of a "smooth" random potential (the condition $V_0 >> E_0$ will be always satisfied if the correlation length R_0 is made large enough). Since,

in contrast to the previous case, the energy E_0 is much below the height of a typical barrier, the condition $kR_0 >> 1$ becomes now the necessary condition for diffusive transport. We start with the Born approximation, which should always hold at sufficiently high energies.

For the case $V_0 >> E_0$, the Born approximation for a potential barrier of strength V_0 and size R_0 results in a scattering cross section

$$\sigma \sim \left(\frac{V_0}{kE_0}\right)^2, \tag{25}$$

and the approximation is valid only if the particle energy satisfies [42]

$$\epsilon >> \frac{V_0^2}{E_0} \equiv E_\Delta. \tag{26}$$

The scattering is strongly anisotropic and the transport cross section σ^* is smaller than σ by a factor $(1/kR_0)^2$, which yields a transport mean free path given in Eq. (17). The latter contains only quantities with a clear classical meaning, and it can be arrived at by purely classical considerations. Consider a particle with an initial velocity v, in a given direction. The particle is subjected to a force of magnitude $|\mathbf{F}| = |\nabla V(\mathbf{r}| \sim V_0/R_0$. The direction of the force is changing randomly, at a distance of order R_0. During a time interval $\triangle t = R_0/v$ the particle will acquire a velocity increment $|\triangle v| \sim F\triangle t/m \sim V_0/mv$. This increment has a random direction, so that the number of time intervals $\triangle t$, needed to completely degrade the initial direction, is of order $(v/\triangle v)^2 \sim (\epsilon/V_0)^2$. Thus, the time after which the initial direction is forgotten (the transport time) is

$$\tau^* \sim \left(\frac{v}{\triangle v}\right)^2 \triangle t \sim \left(\frac{\epsilon}{V_0}\right)^2 \frac{R_0}{v}, \tag{27}$$

and the corresponding mean free path is

$$l^* \sim v\tau^* \sim R_0 \left(\frac{\epsilon}{V_0}\right)^2 \quad , \qquad (\epsilon >> V_0) \tag{28}$$

which coincides with (17). This coincidence was pointed out in [50] and it is quite remarkable, because Born approximation is incompatible with semiclassics [42]. Indeed, the Born scattering cross section, Eq. (25), strongly differs from the semiclassical one, which is of order R_0^2. Also the differential

cross sections are entirely different: the typical scattering angle in the Born approximation is $1/kR_0$, whereas in semiclassics it is $\triangle v/v \sim V_0/\epsilon$. It is only the *transport* scattering cross section (and hence the transport mean free path) that is given by a similar expression in both approaches. Furthermore, for $\epsilon < E_\Delta$ the Born approximation breaks down. The estimate for l^* in Eq. (28), however, holds as long as $\epsilon >> V_0$. Thus, we arrive at the conclusion that the only condition required for a diffusive transport (with (28) serving as an order-of-magnitude estimate for l^*) is $\epsilon >> V_0$, i.e. the particle energy must well exceed the typical hight of the potential barriers. The corresponding diffusion coefficient is

$$D_\epsilon = vl^*/3 \sim D_0(\epsilon/V_0)^{5/2}, \tag{29}$$

where $D_0 = (V_0 R_0^2/m)^{1/2}$ is the natural unit for classical diffusion (this is the only combination, of the three quantities involved, with dimensions of a diffusion coefficient).

When ϵ approaches V_0, the transport mean free path approaches a value of order R_0. The energy interval $\epsilon \sim V_0$ marks a transition from a "soft", small angle scattering to "hard" scattering, when propagation direction changes drastically in a single scattering event (in this case there is no need to distinguish between l and l^*). When the particle energy becomes smaller than V_0, and it is lowered towards the classical percolation threshold, reflection from potential barriers starts to play an important role and serves as "bottleneck" for transport. The transport slows down, because the particle can get temporarily trapped in a small region and it has to make many bounces between the potential barriers before it escapes. Eventually, at some critical energy E_c transport (at zero temperature) comes to complete halt. Classically, such transition to an insulating state would have occurred at the percolation threshold E_{per}, with a diffusion coefficient [51] behaving in the threshold vicinity as $D \sim D_0[(\epsilon/E_{per}) - 1]^t$, where t can be identified with the percolation conductivity exponent, close to 1.7 in $3d$ [31, 52]. Classical treatment, however, is never adequate close to the transition, where quantum interference effects dominate. Thus, when the energy is lowered towards E_{per}, the diffusion coefficient, at first, will behave in accordance with the classical percolation theory but, eventually, a crossover to the quantum (Anderson) transition must take place [53] . This transition occurs at the mobility edge E_c, which is strictly larger than E_{per}. (We stress that this consideration applies only if $V_0 >> E_0$, whereas in the opposite case, considered in the previous subsection, no trace of classical percolation appears in the transport

picture.) The difference $(E_c - E_{per})$ can be roughly estimated by locating the energy at which the classical expression $D_0[(\epsilon/E_{per}) - 1]^t$ gets equal to the "diffusion quantum" $\hbar/m$. Such estimate yields $E_c = E_{per}(1 + \eta^{-1/2t})$.

One can also appreciate the importance of quantum effects, while moving towards E_{per} from the low energy side. Well below E_{per} states are localized, essentially in a single potential well. When ϵ is raised, a state spreads over several wells. At $\epsilon = E_{per}$, a classical particle would get delocalized but quantum interference prevent delocalization. Only when $\epsilon > E_c > E_{per}$, does delocalization become possible.

The above relation between E_c and E_{per} is based on the assumption of two well separated scales: a "microscopic" scale, at which local diffusion (with a diffusion constant D_0) takes place, and a macroscopic one, related to the topology of the percolating cluster and responsible for the "slowing-down factor" $[(\epsilon/E_{per}) - 1]^t$. This assumption is by no means obvious even for the "generic" random potentials, usually assumed in the percolation theory [31, 52]. Moreover, one can construct "unusual" potentials, the extreme example being a potential which, although random, is strictly zero within a connected spatial region. Percolation is then possible at all energies, and there is no connection at all between classical percolation and quantum localization. Actually, a blue detuned speckle might be not so far from this extreme example since, due to the high probability for low values of the potential, the percolation threshold (in $3d$) is only about $4 \cdot 10^{-4} V_0$ [54].

3.3 $d = 2$ and $\eta << 1$

In two dimensions all states are localized. If, however, the disorder (at the given energy) is weak, i.e. $kl >> 1$, the localization length is exponentially large. In this case, in a finite size sample, the wave function can easily spread over the entire sample, and the states can be considered as extended, for all practical purposes. When disordered increases (or the particle energy decreases, for fixed disorder), the localization length becomes smaller and, eventually, the regime of strong localization is reached. Thus, in $2d$, one speaks about a crossover from weak to strong localization, instead of a strict transition between extended and localized states that is taking place in $3d$.

This picture can be rephrased in terms of transport. At high energies the ordinary diffusive transport is possible. Indeed, it would take unrealistically large samples and exponentially long times (in addition to the almost complete absence of any inelastic processes) to find out that the initial wave

packet gets, in fact, localized. Under appropriate conditions, one can observe weak localization corrections, on top of diffusion [55, 33, 35]. When the energy is lowered, the diffusion coefficient decreases and one crosses over to the strong localization regime: the localization length becomes much smaller than the sample size and transport is inhibited.

As in Sec. 3.1, we start with an estimation of the cross section for a single scatterer- a potential barrier of hight V_0 and radius R_0. For a slow particle, $kR_0 << 1$, this cross section in the Born approximation is [42] $\sigma \sim \eta^2/k$ and, unlike the $3d$ case, it is energy dependent. The approximation is valid for $kR_0 >> \eta^2$. Next, we estimate the mean free path for a particle moving in the presence of many scatterers, in concentration $n_{scat} \sim R_0^{-2}$:

$$l = \frac{R_0^2}{\sigma} \sim \frac{kR_0^2}{\eta^2}. \tag{30}$$

Furthermore, the Ioffe-Regel criterion, $kl >> 1$, results in the condition $kR_0 >> \eta$ (this is more restrictive than the condition $kR_0 >> \eta^2$ for a single scatterer). In terms of the particle energy one obtains [27, 56]:

$$\epsilon >> V_0\eta \equiv E_\Delta. \tag{31}$$

This energy scale has already appeared in (26), although its significance here is quite different from that in Sec. 3.2, devoted to the smooth $3d$ potential.

Consider now the fast particles, $kR_0 >> 1$. The transport scattering cross section for those differs from $\sigma \sim \eta^2/k$ by a product of two small factors (compare to the corresponding estimate in Sec. 3.1). The factor $1/kR_0$ accounts for the narrow scattering sector, in the forward direction, and the factor $1/(kR_0)^2$ accounts for the difference between the scattering and the transport cross sections. Thus, $\sigma^* \sim \eta^2/k^4R_0^3$, and the transport mean free path $l^* = R_0^2/\sigma^* \sim R_0(\epsilon/V_0)^2$, as in (17).

The quantitative treatment of l^*, in the Born approximation, is based on the $2d$ counterpart of (18):

$$\frac{1}{\tau^*} = \frac{1}{\hbar} V_0^2 \nu \int_0^{2\pi} d\phi \tilde{\Gamma}\left(2k \sin\frac{\phi}{2}\right)(1 - \cos\phi), \tag{32}$$

where $\nu = m/2\pi\hbar^2$ is the $2d$ density of states and $\tilde{\Gamma}$ is the Fourier transform of the correlation function $\Gamma(R/R_0)$ for the $2d$ random potential. For a

Gaussian correlation function, $\Gamma = \exp(-R^2/R_0^2)$, the result for $l^* = \hbar k\tau^*/m$ is [27, 56, 57]:

$$l^*(\epsilon) = \frac{R_0}{\pi}\left(\frac{\epsilon}{E_0}\right)^{1/2}\left(\frac{2E_0}{V_0}\right)^2 f\left(\frac{\epsilon}{2E_0}\right) \quad , \quad (\epsilon >> E_\Delta). \tag{33}$$

Here the function $f(x) = e^x[I_0(x) - I_1(x)]^{-1}$, where I_0 and I_1 are the modified Bessel functions. For small x, $f(x) \approx 1$; for large x, $f(x) \approx \sqrt{\pi}(2x)^{3/2}$. In these limits of slow and fast particles, respectively, one can immediately write down the corresponding values for the mean free path, in complete agreement with the above estimates. In terms of the diffusion coefficient, $D_\epsilon = vl^*/2$, the limiting values are:

$$D_\epsilon = \begin{cases} \frac{2\hbar}{\pi m}\left(\frac{\epsilon-\overline{V}}{E_\Delta}\right) & , \quad E_\Delta << (\epsilon - \overline{V}) << E_0 \\ (\frac{8V_0R_0^2}{\pi m})^{1/2}\left(\frac{\epsilon-\overline{V}}{V_0}\right)^{5/2} & , \quad \epsilon >> E_0 \end{cases} \tag{34}$$

where, as in (20), we have made it explicit that the energy should be counted from the average potential value.

The important case of a correlation function, corresponding to a speckle potential created by a uniformly illuminated circular diffusive plate, was considered in [27]. Although that correlation function decays only as R^{-3} (with oscillations), the integral $\int \Gamma(\mathbf{R}) d^2R$ is finite, so that this case is, qualitatively, not different from the Gaussian correlation. The equation (34) still holds, albeit with different numerical coefficients (note that our definition of E_0 and η differs by a factor of 2 from that in [27]).

Unlike the $3d$ case, when the condition $(\epsilon - \overline{V}) >> W$ was sufficient for diffusive transport, in $2d$ the condition $(\epsilon - \overline{V}) >> E_\Delta$ is only a necessary one. In an ideal world of infinite samples, infinite times and zero temperature, quantum interference effects would eventually take over and transport would cease. In reality, factors like dephasing or finite sample size suppress interference and provide room for diffusion. Interference effects show up in a correction to the diffusion coefficient (weak localization). As the just mentioned "ideal conditions" are approached, interference becomes more important and the diffusion coefficient approaches zero. All this is discussed in great detail in [26, 27]. For $(\epsilon - \overline{V}) \sim E_\Delta$ a crossover to strong localization takes place. The localization length ξ rapidly decreases with energy, and for $(\overline{V} - \epsilon) >> E_\Delta$ the region of strongly localized states, well separated from

each other, is reached. This region of the spectrum has been already discussed in Sec. 3.1, one should only set $d = 2$ in the corresponding expressions.

In condensed matter physics, transport in the region of strongly localized states can occur only at finite temperatures, and it is due to hopping [31, 58]: an electron can hop from one localized state to another by absorbing a phonon. In principle, one should be able to observe a similar phenomenon for localized cold atoms, by modelling phonons with the help of a random, time-dependent optical potential (this remark applies, of course, also to $3d$).

3.4 $d = 2$ and $\eta >> 1$

A few brief remarks will suffice to summarize the situation for this case. Using considerations entirely similar to those in Sec. 3.2, one can see that Eq. (28) for the transport mean free path is valid also in $2d$, as long as $\epsilon >> V_0$. The corresponding diffusion coefficient is $D = vl^*/2 \sim D_0(\epsilon/V_0)^{5/2}$, i.e. the same as in $3d$, up to a numerical factor.

When ϵ approaches the typical barrier height V_0, the diffusion coefficient reaches a value $\sim D_0$, and it keeps decreasing when the energy is lowered further. The decrease occurs for two reasons: first, it becomes more a more difficult for a (classical) particle to find a path around the potential barriers and, second, the quantum interference effects are being enhanced, leading to strong localization. When D reaches a value of order $\hbar/m$, the classical picture breaks down completely. Diffusion of a classical particle in a $2d$ speckle potential has been numerically studied in [28], and it would be interesting to account for quantum effects, including the classical-quantum crossover.

4 A superfluid-insulator transition in a disordered BEC

The behavior of a BEC in a random environment is a vast subject, with a long history. The question of how disorder can affect, and possibly destroy, superfluidity and superconductivity has been repeatedly discussed in the literature [59, 33]. In particular, Ref. [59] contains a thorough discussion on ^4He absorbed in a porous Vycor glass. The porous, random structure of the medium can lead to a significant reduction of the superfluid transition temperature T_c.

Ultracold atomic gases, which allow for a very accurate control over both the disorder and the interparticle interaction, provide an ideal system for studying the interplay between the two factors. The problem is of fundamental interest, because it brings together two central themes in condensed matter physics: interactions and disorder. In the absence of interactions all bosons would drop into the lowest potential well, so the ideal Bose gas is clearly not the appropriate starting point for the theory. Any finite repulsive interaction has a drastic effect, pushing the particles apart and not allowing for too high local density $n(\mathbf{r})$. If the average particle density, n, is finite, the particles will get spread over the entire (infinite) system.

We will assume the model of a continuous random potential V($\mathbf{r}$) (see previous section), thus, leaving out the work on disordered (or quasiperiodic) optical lattices and the disordered Bose-Hubbard model (see [5] for an extensive discussion and references, and [60, 61] for recent experiments). Furthermore, we will not discuss finite temperature effects or excitations above ground state [54, 62, 63, 64] but focus on the zero-temperature, quantum phase transition, i.e., the transition between a superfluid and an insulator under a change of the chemical potential μ (or the particle density n) [39, 40]. Ref. [40] contains a detailed exposition of various regimes, in $2d$ and $3d$, including the effect of a harmonic trap. We refer the reader to [40] for details, and here only review the transition in $3d$, for a short range random potential, $\eta << 1$.

We consider, thus, N bosons in a box of volume Ω, in the thermodynamic limit ($N, \Omega \to \infty, n = N/\Omega = const$). Repulsive interactions and the "gas condition", $na^3 << 1$, are assumed. Here a is the scattering length, related to the interaction constant as $g = 4\pi\hbar^2 a/m$. In the absence of disorder, the chemical potential is $\mu = gn$ [12, 13]. A weak random potential can be treated in perturbation theory [65, 66]. The important energy, characterizing a short range random potential, is W (see Eq.(16)). A particle with the deBroglie wave length $\lambda_p >> R_0$ experiences not the "bare" potential $V(\mathbf{r})$ but a smoothed, effective potential, and the scattering can be considered weak as long as $\lambda_p << l \sim R_0/\eta^2$. For a BEC the role of λ_p is played by the healing length $\xi_h = \hbar/\sqrt{2mgn} = \hbar/\sqrt{2m\mu}$ and the effect of the potential is small, provided the condition $\xi_h << l$, i.e. $\mu >> W$, is satisfied. Thus, for $\mu >> W$ one has a weakly disordered BEC. It is described by a macroscopic wave function $\Psi(\mathbf{r})$ which, although fluctuating in space, maintains coherence over the entire box. The system is a superfluid.

The perturbation theory is expected to break down when μ reaches a value

of order W, i.e. when particle concentration becomes of order $W/g \sim 1/\mathcal{L}^2 a$, where we have introduced the Larkin length defined in Sec. 3.1. At such concentrations disorder becomes more important, fluctuations grow stronger and at some point the coherence gets disrupted: the superfluidity is destroyed and the system undergoes a transition to the insulating state. Let's denote this critical concentration by n_c and the corresponding value of the chemical potential $\mu = \mu_c$. Generally, there is no simple relation between μ_c and the mobility edge E_c (or the energy W). To determine μ_c one has to solve the many body problem of interacting disordered bosons, whereas E_c is a single particle property. In other words, there is no straightforward connection between superfluidity and the nature of the single-particle states (localized vs extended). Indeed, it has been argued long ago [67] that, due to the interaction induced screening, a condensate can exist when the chemical potential is well below E_c. Nevertheless, an estimate of μ_c for weakly interacting disordered bosons [39, 40] shows that W is an important energy scale in the problem. The arguments and estimates in [39, 40] were made for a Gaussian random potential. Since, however, the main "action" is taking place in a narrow interval near $\overline{V}$, the considerations should apply also to a speckle potential. For small n, when μ (measured from the average potential value $\overline{V}$) is negative and large in the absolute value, the distribution of particles in space is highly inhomogeneous. The particles, in the ground state, fill the potential wells with radius smaller than some value R (the corresponding depth is $\sim -\hbar^2/mR^2$), and the purpose is to determine this value, for a given n. Let's denote by $n_w(R)$ the concentration of such wells. For R small, namely $R << \mathcal{L}$, the typical distance between neighboring wells is exponentially large and their concentration is [40]

$$n_w(R) = \frac{1}{R^3} f\left(\frac{\mathcal{L}}{R}\right) \exp\left(\frac{-\mathcal{L}}{R}\right) , \tag{35}$$

where the preexponent f plays no significant role in the forthcoming estimate. The average number of particles per well is $N_w(R) = n/n_w(R)$ and the particle density in a well is $n_p(R) = 3N_w(R)/4\pi R^3$. The total energy of $N_w(R)$ bosons in such a well is comprised of two parts: the binding energy and the interaction energy. Introducing the energy per particle, $E(R)$, one can write (with somewhat arbitrary numerical coefficients):

$$E(R) = -\frac{\hbar^2}{2mR^2} + gn_p(R) = -\frac{\hbar^2}{2mR^2} + \frac{3\hbar^2 na}{n_w(R)mR^3} . \tag{36}$$

Now, using (35) and minimizing (36) with respect to R (for fixed n), one obtains [40]:

$$R(n) = \frac{\mathcal{L}}{ln(n_c/n)} \quad , \qquad n_c = \frac{1}{3\mathcal{L}^2 a} \; . \tag{37}$$

For this result to be valid, one must require $n << n_c$. On the other hand, since the number $N_w(R)$ must be large, n should be not too small, namely:

$$n_c \exp\left[-(\mathcal{L}/3a)^{1/3}\right] << n << n_c, \tag{38}$$

which is consistent only if $\mathcal{L} >> a$. Under the condition (38), tunneling between the wells is negligible and the number of particles in each well is fixed. The state is insulating (a fragmented condensate). The chemical potential is estimated as

$$\mu(n) \sim -\frac{\hbar^2}{mR^2(n)} \sim -W \ln^2\left(\frac{n_c}{n}\right). \tag{39}$$

When n increases, the size $R(n)$ of the relevant wells gets larger and, for $n \sim n_c$, it becomes comparable to the separation between the wells (both are of order $\mathcal{L}$). Tunneling becomes significant and at some point a transition to the coherent superfluid state occurs. Of course, n_c, as defined in (37), is not the precise transition point but only an order of magnitude estimate. Similarly, the critical value μ_c of the chemical potential is not accurately known.

5 Dynamics of cold atoms in the presence of disorder

The present section is devoted to the time evolution of atomic clouds subjected to a random potential. In a typical experimental set-up a ultracold atomic gas, of either bosons or fermions, is released from a harmonic trap, $V_{tr}(r) = m\omega^2 r^2/2$, and undergoes expansion while being scattered by a random potential $V(\mathbf{r})$. The trap determines the initial state of the gas, whereas the potential $V(\mathbf{r})$ affects its subsequent time evolution. At some moment t an image of the atomic cloud is taken, providing information about the mode of transport. We discuss separately two atomic systems: BEC and a cold Fermi gas.

5.1 Ballistic expansion of a BEC

We start with the problem of a free, ballistic expansion, i.e. the random potential is absent. BEC in the trap is described by a macroscopic wave function, satisfying the stationary Gross-Pitaevskii equation

$$-\frac{\hbar^2}{2m}\triangle\Psi + \frac{1}{2}m\omega^2 r^2\Psi + g|\Psi|^2\Psi = \mu\Psi. \tag{40}$$

Usually, interaction among the atoms in the trap is of great importance: the size of the condensate, $R_\mu \sim (\mu/m\omega^2)^{1/2}$, is much larger than the "oscillator size" $a_0 = (\hbar/m\omega)^{1/2}$. The latter is, roughly, the size of a single particle ground state wave function, and in the absence of interactions all the bosons would have condensed into this single particle state. The inequality $R_\mu >> a_0$ implies $\mu >> \hbar\omega$. This is the condition for validity of the Thomas-Fermi approximation which amounts to the neglect of the kinetic energy term in (40), thus, resulting in a simple expression (an inverted parabola) for the condensate density

$$n(\mathbf{r}, t=0) = |\Psi(\mathbf{r}, t=0)|^2 = \frac{\mu}{g}\left(1 - \frac{r^2}{R_\mu^2}\right) \quad , \qquad R_\mu = \left(\frac{2\mu}{m\omega^2}\right)^{1/2} \tag{41}$$

where we have added the time argument $t = 0$, to emphasize that this is the condensate profile in the trap, prior to its release. The corresponding wave function is a square root of this expression, with an arbitrary overall phase which can be set to zero:

$$\Psi(\mathbf{r}, t=0) = \left[\frac{\mu}{g}\left(1 - \frac{r^2}{R_\mu^2}\right)\right]^{1/2} \equiv F(r). \tag{42}$$

This expression is accurate in the bulk of the condensate, and it breaks down only close to the boundary, for $r \approx R_\mu$.

Assume now that at $t = 0$ the trap potential is switched off, and for $t > 0$ the BEC undergoes free evolution, according to the time dependent Gross-Pitaevskii equation:

$$i\hbar\frac{\partial\Psi}{\partial t} = -\frac{\hbar^2}{2m}\triangle\Psi + g|\Psi|^2\Psi \ , \qquad \int d\mathbf{r}|\Psi|^2 = N. \tag{43}$$

with the initial condition given in (42). The wave function is normalized to the total number of particles N. $\Psi(\mathbf{r}, t)$ is a complex function, $\Psi =$

$\sqrt{n}\exp(i\theta)$, i.e. the condensate acquires a dynamic phase $\theta(\mathbf{r}, t)$. Eq. (43) can be rewritten as a set of two hydrodynamic equations, in terms of the condensate density $n(\mathbf{r}, t)$ and its velocity $\mathbf{v}(\mathbf{r}, t) = (\hbar/m)\nabla\theta(\mathbf{r}, t)$ [12, 13]:

$$\frac{\partial n}{\partial t} + div n\mathbf{v} = 0 \tag{44}$$

$$m\frac{\partial \mathbf{v}}{\partial t} + \nabla\left(\frac{1}{2}mv^2 + gn\right) = 0, \tag{45}$$

where in the second equation the "quantum pressure" term has been neglected, which is justified if the healing length ξ_h is smaller than the characteristic scale over which the density is changing (see the discussion in [13]). These equations have to be solved with the initial conditions $\mathbf{v}(\mathbf{r}, t = 0) = 0$ and $n(\mathbf{r}, t = 0)$ given in (41). The solution is [12, 68, 69]:

$$n(\mathbf{r}, t) = \frac{\mu}{gb^d}\left(1 - \frac{r^2}{b^2 R_\mu^2}\right), \qquad \mathbf{v}(\mathbf{r}, t) = \frac{\dot{b}}{b}\mathbf{r}, \tag{46}$$

where the scaling factor $b(t)$ obeys the ordinary differential equation $\ddot{b} = \omega^2/b^{d-1}$, with $b(0) = 1, \dot{b}(0) = 0$ (a dot on b denotes time derivative). At $d = 2$ its solution is $b(t) = \sqrt{1 + \omega^2 t^2}$, and at $d = 3$ it is qualitatively similar, namely: $b \approx 1$ for $t << 1/\omega$ and $b \approx \omega t$ for $t >> 1/\omega$ (linear evolution).

Thus, in the course of the expansion the condensate density $n(\mathbf{r}, t)$ retains its shape of an inverted parabola whose size increases according to the scaling factor $b(t)$. The important time scale in the expansion process is $t_0 = 1/\omega$. For $t << t_0$ the time evolution is dominated by the nonlinear term in (43) and the condensate energy is due primarily to the interaction. By the time $t \sim t_0$ most of the interaction energy gets converted into the kinetic energy of the condensate flow. The wave function $\Psi(\mathbf{r}, t_0)$ exhibits rapid spatial oscillations which account for the large kinetic energy of the condensate. For $t >> t_0$ the interaction term (i.e. the nonlinear term in (43)) becomes negligible and the wave function evolves according to the linear Schrödinger equation. The function at $t = t_0$ is, roughly,

$$\Psi(\mathbf{r}, t_0) \simeq F(\frac{r}{2})\exp(ir^2/a_0^2) \equiv \Phi(r), \tag{47}$$

where the argument $r/2$ in F indicates that by the time t_0 the condensate's size has increased by a factor of 2 or so. One can check that the kinetic energy in this wave packet, $E_{kin} = \frac{\hbar^2}{2m}\int |\nabla\Psi|^2 d\mathbf{r}$, is of the same order of magnitude as the interaction energy, $E_{int} = \frac{g}{2}\int |\Psi|^4 d\mathbf{r}$.

5.2 Diffusion of a BEC

Here we study the time evolution of a BEC, in a random potential $V(\mathbf{r})$, upon its release from the trap. The evolution is governed by the Gross-Pitaevskii equation, with the random potential:

$$i\hbar\frac{\partial\Psi}{\partial t} = -\frac{\hbar^2}{2m}\triangle\Psi + V(\mathbf{r})\Psi + g|\Psi|^2\Psi \tag{48}$$

Sometimes it is possible to disentangle the effects of nonlinearity and disorder [70, 57]. For instance, one can switch the trap off at $t = 0$, let the condensate freely expand for a time interval of the order of $t_0 = 1/\omega$, and only then switch on the random potential. In this way the evolution is separated into two stages. The first stage, for times $t \sim t_0$, is dominated by the nonlinearity (there is no disorder yet), whereas at the second stage, $t >> t_0$, the nonlinearity can be neglected and the evolution proceeds according to the Schrödinger equation

$$i\hbar\frac{\partial\Psi}{\partial t} = -\frac{\hbar^2}{2m}\triangle\Psi + V(\mathbf{r})\Psi \ , \qquad (t > t_0), \tag{49}$$

with the initial condition $\Psi(\mathbf{r}, t = t_0) = \Phi(r)$, see (47). Setting the start of the second stage at $t = t_0$ is, of course, only a rough estimate (one should wait for a time few times larger than t_0 before switching on $V(\mathbf{r})$) but it does capture the main idea of the two-stage evolution.

In a different set-up, one releases the condensate, at $t = 0$, directly into a random potential (rather than switching on the potential later) and the time evolution for $t > 0$ follows the equation (48). If $V(\mathbf{r})$ is sufficiently weak, one can still argue in favor of a two-stage scenario. During the time $t \sim t_0$ nonlinearity dominates over disorder and the expansion is essentially ballistic (Sec. 5.1). For $t >> t_0$ the nonlinearity is weak and disorder becomes the important factor: the evolution is close to linear, according to (49). Whether a given potential $V(\mathbf{r})$ is weak or strong depends on the wave number k of the relevant component of the condensate wave function. If, for instance, the chemical potential μ in the trap is much larger than the mobility edge E_c, then most of the atoms, upon their release from the trap, will experience weak disorder, because the parameter $k_\mu l$ is large ($k_\mu = \sqrt{2m\mu/\hbar^2}$). On the other hand, spreading of the small-k components might be inhibited by disorder and they will stay localized in the vicinity of the trap. For these components the nonlinearity might remain important for all times. In any case, the first

set-up, i.e., when the potential is switched on after sufficiently long interval of a ballistic expansion, is better suited for the two-stage scenario.

Assuming the validity of this scenario, it remains to study the linear evolution (49), with the initial condition (47). This condition carries information about the initial state of the condensate in the trap and about the first stage of expansion, dominated by the nonlinearity. To simplify the notations, we reset the time t_0 to zero, so that the formal solution of (49) is

$$\Psi(\mathbf{r},t) = \int d\mathbf{R} G(\mathbf{r},\mathbf{R},t)\Phi(\mathbf{R}), \tag{50}$$

where G is the retarded Green's function of the Schrödinger equation (49). The average particle density

$$\overline{n}(\mathbf{r},t) = \overline{|\Psi(\mathbf{r},t)|^2} = \int d\mathbf{R} \int d\mathbf{R}' \overline{G^*(\mathbf{r},\mathbf{R},t)G(\mathbf{r},\mathbf{R}',t)}\Phi^*(\mathbf{R})\Phi(\mathbf{R}'). \tag{51}$$

The product of the Green's functions can be Fourier transformed as

$$\overline{G^*(\mathbf{r},\mathbf{R},t)G(\mathbf{r},\mathbf{R}',t)} = \int \frac{d\varepsilon}{2\pi} \int \frac{d\Omega}{2\pi} e^{-\frac{i\Omega t}{\hbar}} \overline{G^*(\mathbf{r},\mathbf{R},\varepsilon+\frac{1}{2}\Omega)G(\mathbf{r},\mathbf{R}',\varepsilon-\frac{1}{2}\Omega)}\,. \tag{52}$$

The product in (52), for weak disorder, can be calculated in the diagram technique [35]:

$$\overline{G^*(\mathbf{r},\mathbf{R},\varepsilon+\frac{1}{2}\Omega)G(\mathbf{r},\mathbf{R}',\varepsilon-\frac{1}{2}\Omega)} = -2P_\varepsilon(\mathbf{r},\mathbf{R},\Omega) Im\overline{G}(\mathbf{R}-\mathbf{R}',\epsilon), \tag{53}$$

where the diffusion ladder is defined as

$$P_\varepsilon(\mathbf{r},\mathbf{R},\Omega) = \frac{1}{2\pi\nu_\epsilon}\overline{G^*(\mathbf{r},\mathbf{R},\varepsilon+\frac{1}{2}\Omega)G(\mathbf{r},\mathbf{R},\varepsilon-\frac{1}{2}\Omega)} \tag{54}$$

and the average Green's function

$$\overline{G}(\boldsymbol{\rho},\epsilon) = G_0(\boldsymbol{\rho},\varepsilon)e^{-\frac{\rho}{2l_\varepsilon}}, \qquad (\boldsymbol{\rho} = \mathbf{R}-\mathbf{R}'). \tag{55}$$

Here G_0 is the free Green's function and ν_ϵ and l_ϵ are, respectively, the (average) density of states and the mean free path. Putting all the pieces together, we arrive at the following expression for the particle density:

$$\overline{n}(\mathbf{r},t) = -\frac{1}{\pi}\int d\mathbf{R}\int d\boldsymbol{\rho}\int d\epsilon P_\epsilon(\mathbf{r},\mathbf{R},t) Im\overline{G}(\boldsymbol{\rho},\epsilon)\Phi^*(\mathbf{R}+\frac{\boldsymbol{\rho}}{2})\Phi(\mathbf{R}-\frac{\boldsymbol{\rho}}{2}), \tag{56}$$

where the quantum diffusion kernel $P_\epsilon(\mathbf{r},\mathbf{R},t)$ is the Fourier transform of the diffusion ladder $P_\varepsilon(\mathbf{r},\mathbf{R},\Omega)$. Although this result was derived for weak disorder, scaling arguments (as presented e.g. in [33, 71]) suggest that, with the appropriate form for the kernel P, the result is valid also when disorder is strong. Transforming $\overline{G}(\boldsymbol{\rho},\epsilon)$ to the momentum representation, $\overline{G}(\mathbf{k},\epsilon)$, enables us to write

$$\overline{n}(\mathbf{r},t)=-\frac{1}{\pi}\int d\mathbf{R}\int d\mathbf{k}\int d\epsilon P_\epsilon(\mathbf{r},\mathbf{R},t)Im\overline{G}(\mathbf{k},\epsilon)W(\mathbf{k},\mathbf{R}), \tag{57}$$

where the Wigner function is defined as

$$W(\mathbf{k},\mathbf{R})=\frac{1}{(2\pi)^d}\int d\boldsymbol{\rho}e^{i\mathbf{k}\cdot\boldsymbol{\rho}}\Phi^*(\mathbf{R}+\frac{\boldsymbol{\rho}}{2})\Phi(\mathbf{R}-\frac{\boldsymbol{\rho}}{2}). \tag{58}$$

Eq. (57) contains three ingredients: (i)The Wigner function carries information about the initial condition. (ii)The factor $-(1/\pi)Im\overline{G}(\mathbf{k},\epsilon)\equiv A(\mathbf{k},\epsilon)$ is the spectral function. For a free particle it is equal to $\delta(\epsilon-\epsilon_{\mathbf{k}})$, with $\epsilon_{\mathbf{k}}=\hbar^2k^2/2m$ (the "on-shell" relation between the energy and momentum). Disorder broadens the δ-function into a Lorentzian or, if sufficiently strong, into some more complicated shape. (iii) The quantum diffusion kernel propagates a particle, with energy ϵ, from $\mathbf{R}$ to $\mathbf{r}$, in time t.

Eq. (57) simplifies in certain limits. If one uses $\delta(\epsilon-\epsilon_{\mathbf{k}})$ for the spectral function, which can be justified for sufficiently weak disorder, one obtains

$$\overline{n}(\mathbf{r},t)=\int d\mathbf{R}\int d\mathbf{k}P_k(\mathbf{r},\mathbf{R},t)W(\mathbf{k},\mathbf{R}), \tag{59}$$

where $P_k\equiv P_{\epsilon_k}$. This equation appears, in a somewhat different form, in [27] and it has a simple interpretation: The initial distribution in phase space, $W(\mathbf{k},\mathbf{R})$, is propagated in time by the propagation kernel $P_k(\mathbf{r},\mathbf{R},t)$. One can rewrite this equation in terms of the momentum $\mathbf{p}=\hbar\mathbf{k}$, making it look entirely classical. Note, however, that both W and P_k are quantum objects.

Another type of approximation, appropriate for large distances r, is based on neglecting the R-dependence of $P_k(\mathbf{r},\mathbf{R},t)$. For particles which had propagated a distance $r>>R_\mu$, the trap (i.e. the initial size of the cloud R_μ) can be viewed as a "point object" and R can be set equal to zero (the center of the trap). The integral of $W(\mathbf{k},\mathbf{R})$ over $\mathbf{R}$ gives the momentum distribution $|\tilde{\phi}(\mathbf{k})|^2$, where $\tilde{\phi}(\mathbf{k})$ is the Fourier transform of the initial wave function $\Phi(\mathbf{r})$. (57) now reduces to [44]

$$\overline{n}(\mathbf{r},t)=\int\frac{d\mathbf{k}}{(2\pi)^d}|\tilde{\phi}(\mathbf{k}|^2\int d\epsilon P_\epsilon(\mathbf{r},0,t)A(\mathbf{k},\epsilon). \tag{60}$$

A still simpler expression for $\overline{n}(\mathbf{r},t)$ is obtained by combining the two aforementioned approximation, i.e. by equating the spectral function in (60) with $\delta(\epsilon-\epsilon_{\mathbf{k}})$:

$$\overline{n}(\mathbf{r},t)=\int\frac{d\mathbf{k}}{(2\pi)^d}|\tilde{\phi}(\mathbf{k}|^2P_k(\mathbf{r},t), \tag{61}$$

where the second argument, $\mathbf{R}=0$, in $P_k(\mathbf{r},\mathbf{R},t)$ is omitted. The expression (61) can be visualized as dynamical evolution of a cloud of classical particles, which are initially at the origin and whose velocity distribution is determined by $|\tilde{\phi}(\mathbf{k})|^2$. Thus, (61) applies either to a BEC (a single coherent wave packet) or to a cloud of independent, non-interacting particles, e.g., a Fermi gas (see Sec. 5.4). The information about the system is in the initial distribution $|\tilde{\phi}(\mathbf{k})|^2$, which can be, for instance, the thermal distribution (Bose or Fermi) at a given temperature.

The interpretation of $\overline{|\Psi(\mathbf{r},t)|^2}$ in terms of "particles" is not limited to (61) but holds generally. One can imagine performing integration over $\mathbf{R}$ and $\mathbf{k}$ in (57), ending up with the spectral decomposition of the condensate density $\overline{n}(\mathbf{r},t)=\int\frac{d\epsilon}{2\pi}\overline{n}_\epsilon(\mathbf{r},t)$. Similarly, integration over $\mathbf{R}$ and ϵ would produce the momentum decomposition $\int\frac{d\mathbf{k}}{(2\pi)^d}\overline{n}_{\mathbf{k}}(\mathbf{r},t)$. Thus, one can interpret the total density $\overline{n}(\mathbf{r},t)$ as being composed of fictitious particles, or atoms, with a given energy (or momentum), and in what follows we often use this intuitive picture, talking for instance about fast or slow particles. One should keep in mind, though, that the condensate wave function is a coherent unit and that only the total density has the straightforward interpretation in terms of the actual bosonic atoms.

To proceed further one needs an expression for the quantum diffusion kernel $P_\epsilon(\mathbf{r},\mathbf{R},t)$. This is the main object of the theory because it determines the dynamics, for a given ϵ. For weak disorder, when propagation is by simple diffusion, P is the standard diffusion propagator:

$$P_\varepsilon(\mathbf{r},\mathbf{R},t)=\frac{1}{(4\pi D_\varepsilon t)^{d/2}}\exp\left(-\frac{|\mathbf{r}-\mathbf{R}|^2}{4D_\varepsilon t}\right), \tag{62}$$

where D_ε is the (energy dependent) diffusion coefficient (see Sec. 3). When ϵ approaches the mobility edge E_c, the disorder gets stronger and (62) is not applicable any longer. For that case one can use the scaling theory for the Fourier transformed kernel, $P_\varepsilon(\mathbf{r},\mathbf{R},\Omega)$, which is related to the dynamic diffusion coefficient $D_\varepsilon(\Omega)$ [33].

We start with the ordinary diffusion, (62), and restrict ourselves to the long time limit, when (61) is valid. If D were constant, i.e. energy independent, (61) would reduce to a Gaussian function (the momentum distribution is normalized to the total number of particles $\int \frac{d\mathbf{k}}{(2\pi)^d} |\tilde{\phi}(\mathbf{k})|^2 = N$). Due to the energy dependence of D, the shape $\overline{n}(\mathbf{r}, t)$ deviates from Gaussian and it depends on the initial momentum distribution $|\tilde{\phi}(\mathbf{k})|^2$. The characteristic width of this distribution is $k_\mu = \sqrt{2m\mu/\hbar^2} = 1/\xi_h$ and it is due to the rapidly oscillating part which the wave function acquires after the first stage of a ballistic expansion. To a good approximation, in any space dimension, the k-dependence of $|\tilde{\phi}(\mathbf{k})|^2$ is determined by the factor $(1 - \frac{k^2}{2k_\mu^2})$, [68, 69, 27]. For instance, in $2d$

$$|\tilde{\phi}(\mathbf{k})|^2 = \frac{4\pi N}{k_\mu^2} \left(1 - \frac{k^2}{2k_\mu^2}\right) \Theta(k_\mu \sqrt{2} - k). \tag{63}$$

Let us consider a short-range correlated potential, i.e. $\eta << 1$, and assume that $k_\mu R_0 << 1$. It must be also assumed that the chemical potential μ of the condensate (prior to the release from the trap) is much above the mobility edge E_c, so that the great majority of the k-components experience weak disorder and propagate by diffusion. In $2d$ the stated conditions are the same as given in the inequalities in the first line of (34). The mean free time is then independent of k and the diffusion coefficient is $D_k = \hbar^2 k^2 \tau / 2m^2 = D_\mu (k/k_\mu)^2$, where D_μ is the diffusion coefficient for $k = k_\mu$.

The upper limit in the integral (61) is $k_\mu \sqrt{2}$. Since for sufficiently small k diffusion breaks down, a lower cutoff, k_c, should be introduced in the integral. The cutoff is estimated from the condition $kl = 1$ which, using (30), gives $k_c = (\eta/R_0) = (m/\hbar\tau)^{1/2}$. This cutoff is a rough benchmark between the components which diffuse away and those which stay localized. Writing the kernel (62) in terms of k and calculating the integral in (61), with the expression (63) for $|\tilde{\phi}(\mathbf{k})|^2$ and with a lower limit k_c, yields

$$\overline{n}(\mathbf{r}, t) = \frac{N}{4\pi D_\mu t} \left\{ (1 + \alpha) \left[E_1(\alpha) - E_1\left(\frac{2\alpha}{\delta^2}\right) \right] + \frac{1}{2}\delta^2 \exp\left(-\frac{2\alpha}{\delta^2}\right) - e^{-\alpha} \right\}, \tag{64}$$

where $E_1(x)$ is the exponential integral, $\alpha \equiv r^2/8D_\mu t$ and $\delta = (k_c/k_\mu) = \sqrt{\hbar/2\mu\tau}$ is the dimensionless cutoff. The cutoff is important only for small r, to avoid the divergence at $r = 0$. For $r^2 >> \hbar t/m$ the parameter $2\alpha/\delta^2$ is large and the two δ-dependent terms in (64) can be neglected.

In Fig.2 we plot the normalized particle density, $\tilde{n}(\mathbf{r}) = 4\pi D_\mu t \overline{n}(\mathbf{r}, t)/N$, for some fixed time t, as a function of the normalized distance $\tilde{r} = \frac{r}{\sqrt{8D_\mu t}}$.

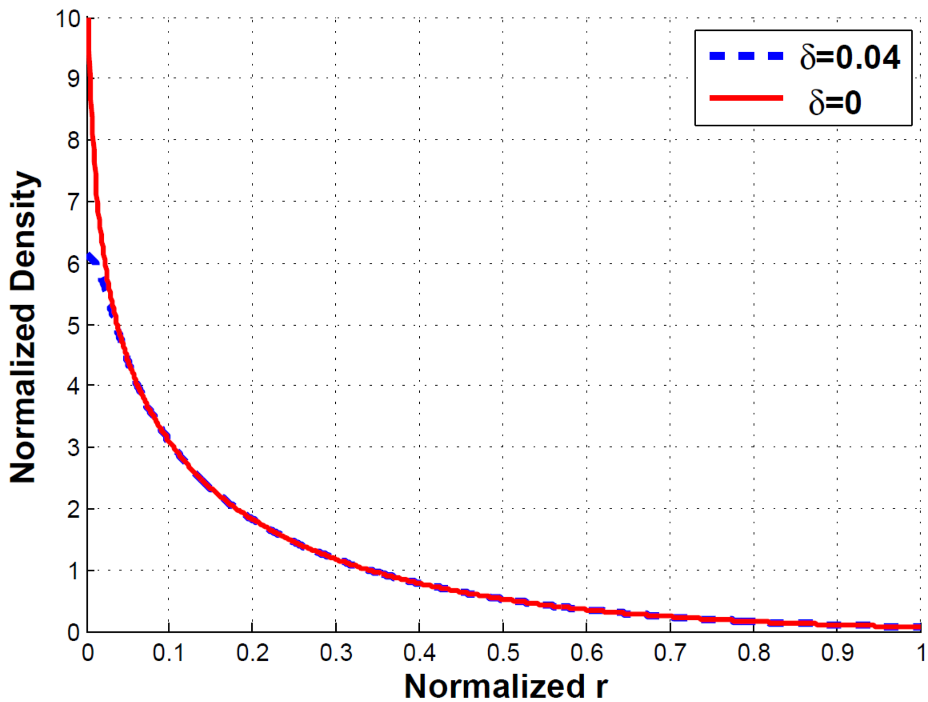

Figure 2: Density as a function of position (both quantities are normalized as explained in the text). The cutoff δ is zero for the solid curve and it is 0.04 for the dashed curve.

The dashed curve corresponds to a cutoff $\delta = 0.04$ while for the solid curve $\delta = 0$. The curves exhibit an exponential tail (with a power-law prefactor) for large $\tilde{r}$. This tail comes from the large-k part of $|\tilde{\phi}(\mathbf{k})|^2$, i.e. from particles which, in a given time, manage to diffuse far away. It can be obtained analytically, using the large-z asymptotics $E_1(z) \approx z^{-1}\exp(-z)$. The sharp increase in $\tilde{n}(\mathbf{r})$ for small $\tilde{r}$ is due to the small-k components whose diffusion coefficient decreases as k^2. Since for small z, $E_1(z) \approx -\ln z$, the solid curve has a logarithmic divergence at the origin. The divergence is rounded off by the finite cutoff δ.

It is sometimes convenient to replace the sharp cutoff in (63) by a smoother, Gaussian cutoff, thus, taking $|\tilde{\phi}(\mathbf{k})|^2 = (4\pi N/k_\mu^2)\exp(-k^2/k_\mu^2)$, with the re-

sult [57]:

$$\overline{n}(\mathbf{r},t) = \frac{N}{2\pi D_\mu t} K_0\left(\frac{r}{\sqrt{D_\mu t}}\right), \tag{65}$$

where K_0 is the zeroth order modified Hankel function, and no lower cutoff δ was introduced. This result is very similar to (63), with $\delta = 0$. Indeed, the function $K_0(z)$ has an exponential tail (with a power-law prefactor) for large z, and it diverges logarithmically for small z.

It is interesting that D_μ is the only system-dependent quantity (except for the total number of atoms N) which appears in (64) or (65). Using the natural quantum unit of diffusion, $\hbar/m$, one can define a dimensionless parameter $mD_\mu/\hbar \sim \mu\tau^*/\hbar$, where τ^* is the transport mean free time for a particle with energy μ (this relation is not restricted to the above $2d$ example). This parameter carries information about the initial state of the condensate (μ depends on the nonlinearity and on other factors), as well as about the subsequent dynamics (via τ^*). It is analogous to the parameter $E_F\tau/\hbar$ which determines the transport properties of a disordered metal (E_F is the Fermi energy).

Diffusion of cold ^{87}Rb atoms, in a $2d$-geometry, was observed experimentally in [9]. Motion in the vertical (z) direction was confined and transport in the x, y-plain was studied. The temperature was somewhat above the condensation temperature, so that instead of the inverted parabola (63) one should use the appropriate thermal distribution [9]. Since the shape of the diffusing cloud is not very sensitive to the precise initial distribution, provided it still contains fast and slow particles, one can expect results similar to those in Fig.2. Indeed, profiles of the (integrated along x or y) density, shown in Fig.3, have clear resemblance with Fig.2. Note the difference between curves in (b) and (c) of Fig.3, for the same propagation time. It is due to the anisotropy in the potential and hence in the diffusion coefficient. The experimental data in [9] were fit numerically to a model with a anisotropic, energy-dependent diffusion coefficient.

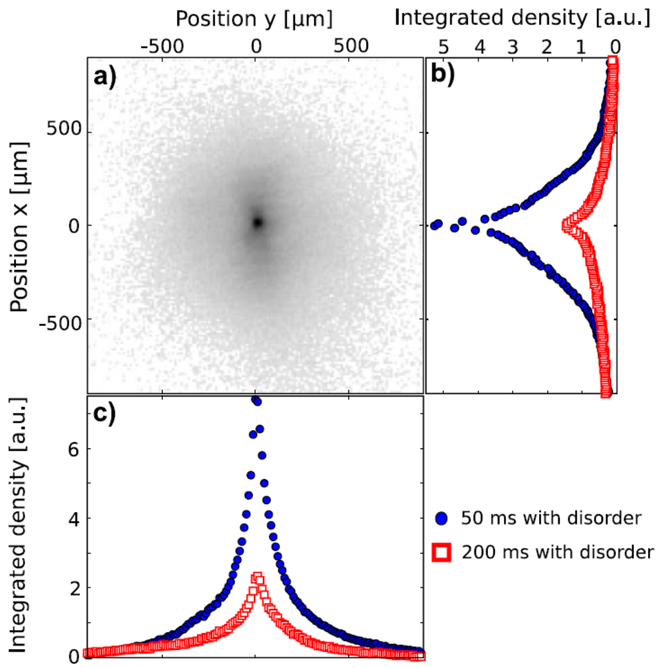

Figure 3: Atomic column density after planar expansion of an ultracold gas in an anisotropic speckle potential. (a) Image after 50 ms of expansion. (b), (c) Integrated density along the two major axes. The plain dots (open squares) correspond to 50 ms (200 ms) of expansion. (Reprinted, with permission, from Phys. Rev. Lett. **104**, 220602 (2010)).

The characterization of a diffusing atomic cloud is not limited to the average particle density $\overline{n}(\mathbf{r},t)$. Indeed, in a *given realization* of randomness the density pattern $n(\mathbf{r},t)$ exhibits spatial fluctuations, which are smoothed out only in the process of averaging over many realizations. The fluctuations are due to multiple scattering of the matter wave on the random potential. The phenomenon is similar to optical speckles for the electromagnetic waves (see Sec. 2) and can be termed "matter wave speckles". The density fluctuations can be described by the (equal time) two point density correlation function, $\overline{n(\boldsymbol{r},t)n(\boldsymbol{r}',t)}$, as well as by higher order correlation functions. The function $\overline{n(\boldsymbol{r},t)n(\boldsymbol{r}',t)}$ reveals both short and long-range correlations, which (for a white noise potential) have been studied, respectively, in [72] and [73].

Finally, let us recall that our discussion has been limited to the "two-stage scenario": first, a free ballistic expansion and only later, when the nonlin-

earity had decreased sufficiently , the disorder is switched on. An interesting and conceptually important question is to what extent the diffusion is modified in the simultaneous presence of disorder and nonlinearity, i.e. when a wave packet evolves according to (48). This problem has been addressed in [74, 75, 76]. It was shown [74] that in the first order in perturbation theory the nonlinearity causes a slight renormalization of the diffusion coefficient which controls the condensate spreading. In the works [75, 76], which went far beyond the simple perturbation theory, a generalized diffusion equation for the spectrally resolved (average) density $\overline{n}_\epsilon(\mathbf{r}, t)$ was derived. The "diffusion coefficient" in that equation depends on $\mathbf{r}$ and t, through the total particle density $\overline{n}(\mathbf{r}, t)$, which has to be determined self-consistently.

5.3 Localization of a BEC

The general expressions (56), (57), derived in the previous subsection, apply also for strong disorder (i.e. when ϵ is in the vicinity, or below the mobility edge E_c), provided one uses the appropriate expressions for the propagation kernel and the spectral function. It is convenient to define the Fourier transform, $P_\epsilon(\mathbf{r}, \Omega)$, of the kernel $P_\epsilon(\mathbf{r}, 0, t) \equiv P_\epsilon(\mathbf{r}, t)$. For ordinary diffusion, (62), $P_\epsilon(\mathbf{r}, \Omega) = (4\pi D_\epsilon r)^{-1} \exp(-r\sqrt{-i\Omega/D_\epsilon})$. More generally,

$$P_\epsilon(\mathbf{r}, \Omega) = \frac{1}{4\pi D_\epsilon(\Omega) r} \exp\left[-r\sqrt{\frac{-i\Omega}{D_\epsilon(\Omega)}}\right], \tag{66}$$

where $D_\epsilon(\Omega)$ is the dynamic, frequency dependent diffusion coefficient which carries information about transport beyond ordinary diffusion. This quantity has been extensively studied in the context of disordered electronic systems, where it is proportional to the *ac* conductivity $\sigma_\epsilon(\Omega)$, with ϵ being the Fermi energy [33, 71]. The $\Omega \to 0$ limit corresponds to the *dc* value. In the localized regime, $\epsilon < E_c$, this value is zero, $D_\epsilon(0) \equiv D_\epsilon = 0$. The dynamic diffusion coefficient, however, is not zero and, for small Ω, it is given by

$$D_\epsilon(\Omega) \sim -i\Omega\xi^2(\epsilon), \qquad (\epsilon < E_c) \tag{67}$$

where ξ is the localization length. Close to the transition $\xi(\epsilon) \propto (E_c - \epsilon)^{-\nu}$, where the exponent $\nu \approx 1.57$ [43]. The expression (67) is easily understood in terms of $\sigma_\epsilon(\Omega)$: although there is no *dc* transport (the eigenstates at energy ϵ are localized), an external field at frequency Ω polarizes the medium, causing an oscillating polarization current.

Note that (67) is valid only for $\Omega < \Omega_c(\xi)$, where the crossover frequency $\Omega_c(\xi)$, estimated below, decreases to zero when $\xi \to \infty$. At the transition point, $\epsilon = E_c$, (67) has no region of applicability and it is replaced by $D_c = (-i\gamma\Omega)^{1/3}$, where γ is a model-dependent coefficient. This behavior follows from the scaling theory of localization [77, 55, 33] and it implies that at the mobility edge a wave packet spreads according to $\overline{r^2} \propto t^{2/3}$ (anomalous diffusion), rather than $\overline{r^2} \propto t$ (ordinary diffusion). Comparing D_c with $D_\epsilon(\Omega)$ in (67) yields $\Omega_c(\xi) \sim \sqrt{\gamma}/\xi^3$, or a characteristic time $t_c = (1/\Omega_c) \propto \xi^3$. This is the crossover time between anomalous diffusion and localization: A particle (a wave packet) with ϵ somewhat below E_c will propagate by anomalous diffusion up to time of order t_c and only then (i.e. after it had spread over a region of size ξ) will it "realize" that it is in fact localized.

A similar crossover occurs at the other side of the transition, $\epsilon > E_c$, where the eigenstates are extended. Close to the transition there exists a macroscopic length $\xi(\epsilon) \propto (\epsilon - E_c)^{-\nu}$, with the meaning of being a crossover length between anomalous and ordinary diffusion. A particle with an energy slightly above E_c first experiences anomalous diffusion, up to a scale $\sim \xi$, and only at a larger scale exhibits ordinary diffusion, with a small *dc* diffusion coefficient $D_\epsilon = 1/\hbar\nu_c\xi \propto (\epsilon - E_c)^\nu$ (here ν_c is the density of states at the energy E_c). Thus, slightly above the transition one can view $D_\epsilon(\Omega)$ as a sum of two contributions: the *dc* part and the anomalous part, proportional to $(-i\Omega)^{1/3}$. On the other hand, well above E_c, where the disorder is weak, the diffusion coefficient (up to small Ω-dependent corrections, responsible for the weak localization effects) is given by the expressions (20) or (29), depending on the value of the parameter η. The existence of a macroscopic length $\xi(\epsilon) \propto (|\epsilon - E_c|^{-\nu}$ on *both* sides of the transition is a consequence of scaling and it is quite natural: only by observing the system at a scale larger than ξ can one distinguish between localized and extended states. Using the expressions for $D_\epsilon(\Omega)$ in various limits, and possibly extrapolating between them, one can reconstruct, via (66), the quantum diffusion kernel $P_\epsilon(\mathbf{r}, t)$. A useful interpolation scheme is the self-consistent theory [38], employed in the numerical part of [44]. Its drawback, though, is that it yields a wrong value for the exponent ν (1 instead of approximately 1.57, in 3d).

In order to use (60) one has to know the spectral function, in addition to the quantum diffusion kernel. The average Green's function, in the momen-

tum representation, can be written as [35] (the Dyson equation):

$$\overline{G}(\mathbf{k},\epsilon) = \frac{1}{\epsilon - \epsilon_{\mathbf{k}} - \sum(\mathbf{k},\epsilon)} \quad , \tag{68}$$

where $\sum(\mathbf{k},\epsilon)$ is the self-energy. The simplest approximation for the self- energy is the first order Born approximation: $\sum(\mathbf{k},\epsilon) = V_0^2 \int (2\pi)^{-3} d^3k' \tilde{\Gamma}(\mathbf{k} - \mathbf{k}') G_0(\mathbf{k}',\epsilon)$, where $\tilde{\Gamma}(\mathbf{q})$ is the Fourier transform of the potential correlation function $\Gamma(\mathbf{R}/R_0)$ and $G_0(\mathbf{k},\epsilon)$ is the unperturbed (i.e. in the absence of disorder) Green's function. A more elaborate approximation is the self-consistent Born approximation, which amounts to replacing $G_0(\mathbf{k},\epsilon)$ by the full Green's function, (68), thus, obtaining a closed equation for the self-energy:

$$\sum(\mathbf{k},\epsilon) = V_0^2 \int \frac{d^3k'}{(2\pi)^3} \frac{\tilde{\Gamma}(\mathbf{k}-\mathbf{k}')}{\epsilon - \epsilon_{\mathbf{k}'} - \sum(\mathbf{k}',\epsilon)}. \tag{69}$$

The solution of this equation is, obviously, an even function of V_0. Therefore the self-consistent Born approximation is hardly appropriate for the speckle potential, where the odd powers of V_0 are known to be generally important [26]. An analytic solution of (69) can be obtained [44] in the limit of a short range potential, when $V_0^2\Gamma(\mathbf{R}/R_0)$ can be replaced with $u\delta(\mathbf{R})$, so that $\tilde{\Gamma}(\mathbf{k}-\mathbf{k}') = u$. The constant u is proportional to $V_0^2 R_0^3$ and the formal limit $V_0 \to 0, R_0 \to \infty, V_0^2 R_0^3 = const$ is implied. For instance, for $\Gamma = exp(-R^2/R_0^2)$ (see Sec. 3.1), $u = \pi\sqrt{\pi} V_0^2 R_0^3$. The solution of (69), with $\tilde{\Gamma}(\mathbf{k}-\mathbf{k}') = u$, yields a $\mathbf{k}$-independent self-energy

$$\sum(\epsilon) = \epsilon^* + \frac{\hbar^2}{8ml^2} - \frac{i\hbar}{2\tau_\epsilon} \quad . \tag{70}$$

The value of ϵ^* depends on the ultraviolet cutoff, needed to regularize the integral in (69). For small but finite correlation radius R_0 the natural cutoff is $1/R_0$, which, in the leading order in the small parameter η, yields $\epsilon^* \sim -\eta V_0$. The mean free path (in $3d$) is $l = \pi\hbar^4/mu^2$ and it does not depend on ϵ. This expression for l is entirely consistent with the result $l = 4R_0/\eta^2\sqrt{\pi}$ of Sec. 3.1 (see the line below (19)), if one substitutes the value $u = \pi\sqrt{\pi}V_0^2 R_0^3$. The mean free time τ_ϵ is related to l in the usual way, $\tau_\epsilon = ml/\hbar k$, with $\hbar k = \sqrt{2m(\epsilon - \epsilon^*)}$. From the condition $kl = 1$ one obtains for the mobility edge $E_c = \epsilon^* + (\hbar^2/2ml^2)$. For η small, E_c is negative (see the corresponding remark in Sec. 3.1). In what follows we set $\epsilon^* = 0$ (the edge of the spectrum)

and count all the energies from this point. The mobility edge becomes $E_c = \hbar^2/2ml^2$.

Knowledge of the self-energy enables us to write down the expression (68) for $\overline{G}(\mathbf{k}, \epsilon)$, and hence for the spectral function

$$-\frac{1}{\pi} Im\overline{G}(\mathbf{k}, \epsilon) \equiv A(\mathbf{k}, \epsilon) = \frac{1}{\pi E_c} \frac{\sqrt{x}}{(x - \frac{1}{4} - \frac{\hbar^2 k^2}{2mE_c})^2 + x} \ , \qquad x = \frac{\epsilon}{E_c}, \quad (71)$$

where, instead of ϵ, the dimensionless variable x has been introduced.

Let us fix some distant point $\mathbf{r}$ and observe the atoms arriving at this point in the course of time, according to (60). If the mobility edge E_c is well below the chemical potential μ (recall that information about μ in (60) is carried by the momentum distribution $\tilde{\phi}(\mathbf{k})$), then $\overline{n}(\mathbf{r}, t)$, as a function of time, will exhibit several regimes. First, the fastest atoms will arrive, by ordinary diffusion (Sec. 5.2) and the density will reach a maximum at a time $t_{arrival} \simeq (r^2/6D_\mu)$. Later, slower particles, with ϵ closer to E_c, will show up. Still later, the anomalously diffusing particles will make their appearance and, finally, for times much larger than the characteristic time $t_{loc} \simeq (\hbar r^3/E_c l^3)$ only the localized part of the condensate will remain. All this has been studied in some detail in [44]. We discuss only the $t \to \infty$ limit, when only the localized part of the condensate is left, at any finite $\mathbf{r}$. In this limit $D_\epsilon(\Omega)$ is given by (67) which, upon substitution into (66) and Fourier transforming with respect to Ω, yields the kernel

$$P_\epsilon(\mathbf{r}, \mathbf{R}, t \to \infty) = \frac{1}{4\pi|\mathbf{r} - \mathbf{R}|\xi^2} \exp\left(-\frac{|\mathbf{r} - \mathbf{R}|}{\xi}\right). \quad (72)$$

The density $\overline{n}(\mathbf{r}, t \to \infty) \equiv \overline{n}_{loc}(\mathbf{r})$ is then obtained from (57) by cutting the upper limit of the integral over ϵ at $\epsilon = E_c$. Since close to E_c the localization length $\xi(\epsilon)$ is large, the localized part of the condensate exhibits long tails. For r well away from the initial location of the condensate, and making use of (71), one obtains [44]:

$$\overline{n}_{loc}(\mathbf{r}) \sim f(E_c/\mu) \frac{N}{r^3} \left(\frac{l}{r}\right)^{1/\nu}, \quad (73)$$

where $f(z) \sim z^{3/2}$ for $z << 1$ and $f(z)$ approaches a constant for $z >> 1$. This localized tail contains information about the localization length exponent ν.

An important quantity is the (average) number of localized atoms, $\overline{N}_{loc}$, or the fraction of the condensate, N_{loc}/N, which remains localized after the mobile part had diffused away. The expression for $\overline{N}_{loc}$ is derived from (57), by integrating it over $\mathbf{r}$ and setting the upper limit in the integral over ϵ at E_c. Since integration of the kernel $P_\epsilon(\mathbf{r}, t)$ over $\mathbf{r}$ gives unity, one obtains

$$\overline{N}_{loc} = \int \frac{d\mathbf{k}}{(2\pi)^d} |\tilde{\phi}(\mathbf{k}|^2 \int_{-\infty}^{E_c} d\epsilon A(\mathbf{k}, \epsilon). \tag{74}$$

In view of the importance of this equation we give an independent, and rather general, derivation. Denoting by $\epsilon_\alpha, |\alpha>$ the energy eigenvalues and eigenvectors for a given realization of disorder, one can write $\Psi(\mathbf{r}, t) \equiv <\mathbf{r}|\Psi> = \sum_\alpha <\mathbf{r}|\alpha><\alpha|\Phi> exp(-i\epsilon_\alpha t)$, where Φ is the initial wave function. In the $t \to \infty$ limit, for any fixed value of $\mathbf{r}$, only localized eigenstates contribute to this expression. Taking its square modulus, integrating over $\mathbf{r}$ and using the orthonormality of the α-basis, yields a simple, intuitively obvious expression for the number of localized atoms $N_{loc} = \sum' | <\alpha|\Phi> |^2$, where the prime indicates that the summation is over localized states only. This expression can be written as

$$N_{loc} = \int_{-\infty}^{E_c} d\epsilon \sum_\alpha \delta(\epsilon - \epsilon_\alpha) <\Phi|\alpha><\alpha|\Phi> = -\frac{1}{\pi} \int_{-\infty}^{E_c} d\epsilon <\Phi| Im\hat{G}(\epsilon)|\Phi>, \tag{75}$$

where $\hat{G}(\epsilon) = (\epsilon - \hat{H})^{-1}$ is the resolvent operator (for the given disorder realization). Writing (75) in the momentum representation and averaging over the disorder results in Eq. (74). $|\tilde{\phi}(\mathbf{k})|^2$ in this equation is a function of k/k_μ. It assumes a constant value $\sim N/(k_\mu)^3$ for $k << k_\mu$, with a cutoff at $k \sim k_\mu$. Furthermore, $A(\mathbf{k}, \epsilon)$, as a function of k, decays on a scale $k_c \sim \sqrt{2mE_c}/\hbar$ (see (71)). It follows then from (74) that N_{loc} is a function of the parameter k_μ/k_c (or μ/E_c). We will not compute the detailed shape of this function but rather analyze the two limits:

(i) $k_\mu >> k_c$. In this case the effective region of integration is $k \sim k_c$, so that the function $|\tilde{\phi}(\mathbf{k})|^2$ can be replaced by its value at $k = 0$, and the remaining integral over $\mathbf{k}$ gives the density of states $\nu(\epsilon)$, i.e.

$$N_{loc} = |\tilde{\phi}(k = 0)|^2 \int_{-\infty}^{E_c} d\epsilon \nu(\epsilon) \sim N(k_c/k_\mu)^3. \tag{76}$$

The fraction of localized atoms $N_{loc}/N << 1$.

(ii) $k_\mu << k_c$. Now the spectral function is "flat" in the effective integration region, $k < k_\mu$, and $\mathbf{k}$ in $A(\mathbf{k}, \epsilon)$ can be set to 0. The remaining integral over $\mathbf{k}$ in (74) is equal to N, by normalization, and using (71), one obtains:

$$\frac{N_{loc}}{N} \equiv f_{loc} = \frac{1}{\pi} \int_0^1 dx \frac{\sqrt{x}}{(x + \frac{1}{4})^2} \approx 0.45. \qquad (77)$$

This result is surprising since the natural expectation is that, in the limit of strong disorder, the fraction of localized atoms should approach unity. A short discussion of this result is given in [44]. The issue deserves further investigation, especially since (71) becomes doubtful in the strong disorder limit.

Recently an experimental observation of Anderson localization of a BEC in $3d$ has been reported [11]. A dilute ^{87}Rb condensate was released from an optical trap and allowed to freely expand for a time $t_0 = 50ms$. After that time the random speckle potential was suddenly switched on and the dynamics of the condensate in that potential has been studied, i.e. images of the atomic cloud at various times have been taken. In Fig. 4 two sequences of images are shown (the time is measured from the instance when the disorder was switched on). The upper sequence corresponds to weak disorder, when a large fraction of the condensate evolves by diffusion. In the lower sequence disorder is strong and a significant fraction of atoms remains localized.

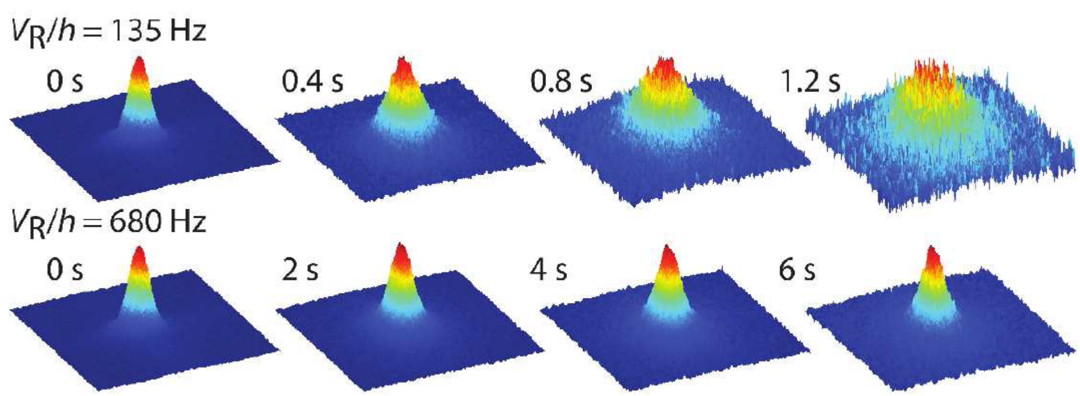

Figure 4: $3d$ expansion of the atomic cloud for the two values of the disorder amplitude. For small disorder ($V_0/h = 135Hz$) one observes an essentially diffusive time evolution. For larger disorder ($V_0/h = 680Hz$) a significant fraction of atoms remains localized. (Reprinted from the arXiv: 1108.0137.)

The theory presented in [11] starts with the following expression for the average density of atoms:

$$\overline{n}(\mathbf{r},t) = \int d\mathbf{R} \int d\epsilon P_\epsilon(\mathbf{r},\mathbf{R},t) D(\mathbf{R},\epsilon) \quad , \tag{78}$$

where the function $D(\mathbf{R},\epsilon)$ is interpreted as the semiclassical density in the position-energy space. Note that with $D(\mathbf{R},\epsilon) \equiv \int d\mathbf{k} W(\mathbf{k},\mathbf{R}) A(\mathbf{k},\epsilon)$ Eq. (78) is compatible with (57). For strong disorder, $E_c >> \mu$, the spectral function is a broad, slowly decaying function of k, and it can be replaced by its k-zero value, $A(k=0,\epsilon) \equiv f(\epsilon)$. The remaining integral over $\mathbf{k}$ gives the initial (i.e. at time t_0) density $n_0(\mathbf{r})$, so that $D(\mathbf{R},\epsilon) = n_0(\mathbf{r}) f(\epsilon)$. A further approximation made in [11] was to replace $P_\epsilon(\mathbf{r},\mathbf{R},t)$ by $\delta(\mathbf{r}-\mathbf{R})$, thus, obtaining for the localized part of the condensate

$$\overline{n}_{loc}(\mathbf{r}) = n_0(\mathbf{r}) \int_{-\infty}^{E_c} d\epsilon f(\epsilon) \equiv n_0(\mathbf{r}) f_{loc} \quad , \tag{79}$$

which is just the initial density profile, rescaled by the factor f_{loc}. The function $f(E)$ was calculated in [11] numerically by diagonalizing the Hamiltonian, for the realistic anisotropic speckle potential, and averaging over several realizations. A value $f_{loc} \approx 0.22$ was obtained, in the strong disorder limit (compare to 0.45 in (77), for the white noise disorder), and after some heuristic energy shift a fair agreement with the experimental results was achieved. Quantitative theoretical results are quite sensitive to various approximations made and, in particular, we note that replacing $P_\epsilon(\mathbf{r},\mathbf{R},t)$ by $\delta(\mathbf{r}-\mathbf{R})$, which might be reasonable for strongly localized states, will break down close to E_c where the localization length becomes large. Therefore (79) for the localized density profile cannot be the full story: $\overline{n}(\mathbf{r}, t \to \infty)$ should have power law decaying tails (see (73)), associated with energies close to E_c.

Let us also mention a different type of localization, which takes place in the momentum space, rather than in real space. When a quantum system (chaotic in the classical limit) is "kicked" by a sequence of short pulses, the expectation value of the momentum square, $< p^2(t) >$, evolves in time. In the well studied kicked rotor model $< p^2(t) >$ saturates in the long time limit [78]- a phenomenon known as dynamical localization, which was observed experimentally in a system of cold atoms [79]. A $3d$ extension of the model [80] exhibits a richer behavior, analogous to the Anderson transition: Depending on the kicking strength, K, $< p^2(t) >$ can either linearly grow with

time (diffusion), saturate in the long time limit (dynamical localization) or display the above mentioned anomalous diffusion, $< p^2(t) > \propto t^{2/3}$ (critical behavior at the Anderson transition point). The latter occurs at a critical value, K_c, of the kicking strength. Such "dynamical Anderson transition" has been experimentally observed in [81, 82, 83]. A system of cold cesium atoms was acted upon by a pulsed laser wave. The authors have identified the transition point K_c, measured the localization parameter, $(K_c - K)^{-\nu}$, close to the transition, and extracted the value of the exponent ν, in very good agreement with the accepted numerical value.

5.4 Cold Fermi gas

Cold Fermi gases are also of interest, as reviewed in [84, 85]. Although interaction between the fermions are generally important, in some cases they have only a minor effect on the dynamics of the atomic cloud. This is particularly true for a polarized Fermi gas when the Pauli principle suppresses the main mechanism (the s-scattering) for the interaction. In this subsection we briefly review some phenomena pertaining to the expansion of a cold Fermi gas released from a harmonic trap.

In the trap, the fermions occupy the single-particle states, $\phi_n(\mathbf{R})$, of the harmonic oscillator potential $m\omega^2 R^2/2$. The derivation of the expression for the average particle density $\overline{n}(\mathbf{r}, t)$ proceeds as in Sec. 5.2. The only difference is that, instead of the condensate wave function $\Phi(\mathbf{R})$, we now have N incoherent single-particle contributions. At zero temperature, when the fermions occupy states up to the Fermi energy E_F, the corresponding Wigner function is

$$W_F(\mathbf{k}, \mathbf{R}) = \frac{1}{(2\pi)^d} \Theta\left(E_F - \frac{\hbar^2 k^2}{2m} - \frac{1}{2} m\omega^2 R^2\right), \tag{80}$$

and the dynamics of the gas, upon its release from the trap, is described by (57), with $W_F(\mathbf{k}, \mathbf{R})$ instead of $W(\mathbf{k}, \mathbf{R})$. In particular, for weak disorder, when the spectral function can be approximated by $\delta(\epsilon - \epsilon_{\mathbf{k}})$, one obtains [86]

$$\overline{n}(\mathbf{r}, t) = \int d\mathbf{R} \int \frac{d\mathbf{k}}{(2\pi)^d} P_k(\mathbf{r}, \mathbf{R}, t) \Theta\left(E_F - \frac{\hbar^2 k^2}{2m} - \frac{1}{2} m\omega^2 R^2\right), \tag{81}$$

which is the precise analog of (59). Diffusion of a Fermi cloud in a $2d$ speckle potential was analyzed in [86]. The authors used (81) with the diffusion

propagator (62) and with D_ϵ appropriate for the $2d$ speckle [27]. The density profile $\overline{n}(\mathbf{r},t)$ turns out to be very similar to that for a diffusing BEC (compare (64) of Sec. 5.2 with Eq.(26) in [86]). This coincidence is not surprising because the Wigner function (80) for fermions has much in common with that for a BEC . Indeed, integrating (80) over $\mathbf{R}$ produces, in $2d$, the momentum distribution $|\tilde{\phi}(\mathbf{k}|^2 = (a_0^4/4\pi)(k_F^2 - k^2)$, where $k_F^2 = 2mE_F/\hbar^2$ and $a_0 = (\hbar/m\omega)^{1/2}$ is the "oscillator size". Similarly, integration over $\mathbf{k}$ results in an inverted parabola $(1/4\pi a_0^4)(R_F^2 - R^2)$ for the initial density of the cloud ($R_F^2 = 2E_F/m\omega^2$). Thus, both the density and the momentum distributions have the same shape as for a BEC in a harmonic trap, see, respectively, (41) and (63). In $3d$ the shapes, although somewhat different, are qualitatively similar. The treatment in [86] can be easily extended to finite temperature T if one uses in (81), instead of the step function, the expression $\{exp[\beta(\frac{\hbar^2k^2}{2m} + \frac{1}{2}m\omega^2R^2 - \mu)] + 1\}^{-1}$, where $\beta = 1/k_BT$.

The problem of localization, as reviewed in Sec. 5.3, should apply, with slight modifications, also to the Fermi gas. So far, however, no specific calculations along these lines have been done. On the experimental side, $3d$ localization of a Fermi gas has been observed in [10], where a gas of ^{40}K was released from a harmonic trap into a speckle potential. According to the authors of [10] their speckle potential is well described by a anisotropic Gaussian autocorrelation function (rather than by the more complicated function in Eq. (8)). The gas was spin polarized, in order to make the interatomic interactions negligible. The temperature range was between 200 and 1500nK, well above the Fermi energy, so that quantum degeneracy played no role. Upon release from the trap, some part of the atomic cloud had diffused away and the remaining localized component was observed. Again, as for the BEC [11], the present state of the theory of Anderson localization in a anisotropic $3d$ speckle potential does not allow for a detail comparison with the experiment.

It is worthwhile to emphasize that the notion of the average particle density $\overline{n}(\mathbf{r},t)$ involves two kinds of averaging. First, one performs the quantum (or thermal) average, i.e. writes down the expectation value $\langle\hat{n}(\mathbf{r},t)\rangle$ of the density operator $\hat{n}(\mathbf{r},t)$, for a given realization of the random potential. Then averaging over the statistical ensemble of realizations is performed, yielding $\overline{\langle\hat{n}(\mathbf{r},t)\rangle} \equiv \overline{n}(\mathbf{r},t)$ [87] (In [86] this quantity is denoted as $n(\mathbf{r},t)$, without the overbar). One should keep in mind, as has been particularly emphasized in [88, 89], that in a single imaging experiment (with sufficient resolution) one does not measure the expectation value $\langle\hat{n}(\mathbf{r},t)\rangle$ but rather one particular event, i.e. some particular density pattern, $n(\mathbf{r},t)$, whose probability

is dictated by the many-body wave function of the system. Therefore even in the absence of disorder a single experimental image will look "noisy" and grainy. (Only upon averaging over many measurements, taken under identical experimental conditions, will one obtain the quantum expectation value $\langle \hat{n}(\mathbf{r},t)\rangle$.) Fluctuations and correlations in such noisy density patterns are characterized by the (equal time) correlation function $\langle \hat{n}(\mathbf{r},t)\hat{n}(\boldsymbol{r}',t)\rangle$. For a clean, homogeneous Fermi gas, in equilibrium, this correlation function is described, for instance, in [90]. It exhibits decaying oscillations, with a characteristic spatial period $\Delta x_0 \sim k_F^{-1}$. Such oscillatory behavior occurs also in a gas confined to a harmonic trap. When the gas is released from the trap, it expands ballistically (in the absence of disorder). The size of the atomic cloud grows linearly with time and so does the correlation length $\Delta x(t) \approx \omega t \Delta x_0$. (In $1d$, an exact expression for the correlation function of a freely expanding Fermi gas has been obtained in [91].) Thus, the free (ballistic) expansion amplifies the scale of correlations.

It has been shown in [72] that in the presence of a random potential, i.e. when the expansion is diffusive instead of ballistic, the picture is different: the size of the atomic cloud grows as $\sqrt{t}$ whereas the (short-range) correlations do not get amplified at all. The authors studied the density-density correlation function

$$C(r,r',t) \;=\; \overline{\langle \hat{n}(r,t)\hat{n}(r',t)\rangle} \,-\, \overline{n}(r,t)\overline{n}(r',t) \,-\, \delta(r-r')\overline{n}(r,t)\,, \quad (82)$$

where the last term describes trivial correlations, which exist already in a classical ideal gas and which are commonly subtracted, in order to isolate the non-trivial correlations [90]. Here we only present an approximate analytic expression for the normalized correlation function in a $3d$ gas (at zero temperature):

$$\frac{C(r,r',t)}{\overline{n}(\boldsymbol{r},t)\overline{n}(\boldsymbol{r}',t)} \;=\; -\frac{9}{g_s}e^{-\Delta r/l_F}\,\frac{\left[\sin(k_F\Delta r)\,-\,(k_F\Delta r)\cos(k_F\Delta r)\right]^2}{(k_F\Delta r)^6}\,, \quad (83)$$

where g_s is the spin degeneracy factor, l_F is the mean free path at the Fermi energy, and $\Delta r = |\boldsymbol{r}-\boldsymbol{r}'|$. The corresponding expression for the $2d$ case can be found in [72].

It is quite remarkable that, while the atomic cloud keeps expanding, the normalized correlation function, (83), does not depend on time. The characteristic length of oscillations remains the same as for the gas in the trap, in sharp contrast with the ballistic case, where the spatial oscillation period is

growing linearly with time. The peculiar behavior of correlations in a diffusively expanding gas is related to phase randomization of the wave function of a diffusing particle. Eq. (83) implies that, as the expansion proceeds, the Fermi gas becomes less "rigid" [72], in the sense that the relative particle number fluctuation increases and approaches the Poisson limit.

6 Free expansion from a disordered trap

So far we have discussed two types of problems: The disordered BEC ground-state, with the ensuing insulator-superfluid transition (Sec. 4), and transport of cold atoms released from a trap into a random potential (Sec. 5). In the present section we consider a different set-up: The trapping potential $V_{tr}(\mathbf{r})$ and the random potential $V(\mathbf{r})$ coexist in the same spatial region, and the atoms are allowed to reach equilibrium in the combined potential. Then, at $t = 0$, *both* potentials are switched off and the atomic system undergoes a free expansion. We discuss in some detail the case of a strongly anisotropic BEC, in a wave guide geometry, and towards the end briefly mention some other cases. Our discussion closely follows Ref. [92].

The BEC is initially strongly confined in the radial direction, $\boldsymbol{\rho}$, by a harmonic trap of frequency $\omega_\perp$. Weak confinement in the axial direction (z) is not essential for our considerations and will be neglected. Thus, prior to its release the condensate is in the ground state (we assume zero temperature), corresponding to the radial confinement potential $\frac{1}{2}\omega_\perp^2\rho^2$ and a z-dependent potential $V(z)$. The latter can be random or deterministic, with characteristic amplitude V_0 and scale of variation $R_0 \equiv 1/k_0$. We assume a weak, smoothly varying potential, in the sense that $V_0 << \mu$ and $k_0 a_\perp << 1$, where $a_\perp = \sqrt{2\mu/m\omega_\perp^2}$ is the radius of the BEC in the trap. The chemical potential μ is assumed to be much larger than $\hbar\omega_\perp$. Under these conditions the Thomas-Fermi approximation is justified and the ground state density is

$$n_0(\rho, z) = \frac{1}{g}\left(\mu - V(z) - \frac{1}{2}m\omega_\perp^2\rho^2\right) . \tag{84}$$

At time $t = 0$ all potentials are switched off and the condensate expands according to the equations (44), (45). These equations are to be solved with the initial conditions (84) for the density and $\mathbf{v} = 0$ for the velocity field. The condensate rapidly expands in the radial direction but, due to the initial density modulation, it also develops an axial velocity component $v_z(z, t)$ and

the related phase. Upon completion of the first stage of the expansion, at time of the order of $t_0 = 1/\omega_\perp$, the phase imprinted on the condensate is [93]

$$\theta(z) = \frac{\pi}{2\hbar\omega_\perp} V(z). \tag{85}$$

During the second stage of the expansion, for times $t >> t_0$, this phase imprint can lead to large density mudulation, of the order or larger than μ, including the possible formation of matter wave caustics. Since we are interested in large effects of this kind, we can neglect from now on the weak initial density modulation (its crucial part was to produce the phase imprint $\theta(z)$). The second stage of the expansion amounts to linear evolution of the BEC wavefunction with the imprinted phase. The wavefunction can be factorized into radial and axial parts, $\Psi(\rho, z, t) = \Phi(\rho, t)\psi(z, t)$, and we are interested in $|\psi(z, t)|^2$, which gives the density at point z and time t, normalized by the radial factor $|\Phi(\rho, t)|^2$. The function $\psi(z, t)$ satisfies the linear, time-dependent Schrödinger equation, with the initial condition $\psi(z, t_0) = \mathrm{e}^{\mathrm{i}\theta(z)}$, whose solution is

$$\psi(z, t) = \sqrt{\frac{m}{2\pi\mathrm{i}\hbar t}} \int \mathrm{d}z' \; \exp\left[\frac{\mathrm{i}m}{2\hbar t}(z - z')^2 + \mathrm{i}\theta(z')\right] , \qquad (t >> t_0) \tag{86}$$

where the impressed phase $\theta(z)$ can be an arbitrary function of z. The typical variation, $\theta_0 = V_0/\hbar\omega_\perp$, of the imprinted phase is the important parameter. In the case $\theta_0 << 1$, implicitly assumed in [93], relative density variations remain small for all times, as is clear from expanding the factor $\exp \mathrm{i}\theta(z')$ in the integrand of Eq (86). Large effects, however, occur in the opposite case, $1 << \theta_0 << \mu/\hbar\omega_\perp$ (the latter inequality stems from the requirement $V_0 << \mu$).

We shall concentrate on the large θ_0 case, and the purpose is to find the form of the relative density $|\psi(z, t)|^2$ at a given instant t. This gives the z-dependence of the density of an expanding atomic cloud, measured with a probe beam perpendicular to the condensate axis. The problem is analogous to the phase screen model in optics, studied extensively by Berry [94]. In that model a monochromatic plane wave encounters a thin screen. The screen impresses on the wave a phase which may be deterministic or random. For strong variation of this phase the wave passing through the screen will develop large intensity variations. Observation of the wave intensity at a point sufficiently far beyond the screen will reveal a pattern of bright lines (caustics). Although the arrangement we consider differs substantially from

that in optics (the corresponding matter wave is not at all monochromatic, the mechanism of impression of the phase is different, and time assumes the role of the spatial axis of propagation in optics), the mathematical treatment of the two problems is essentially the same.

Before discussing the random case, it is instructive to consider a sinusoidal modulation $\theta(z) = \theta_0 \cos k_0 z$. We introduce the dimensionless variables $\tilde{z} = k_0 z$ and $\tilde{t} = t/t^*$, with $t^* = m/\hbar k_0^2 \theta_0$, and rewrite (86) as

$$\psi(\tilde{z},\tilde{t}) = \sqrt{\frac{\theta_0}{2\pi \mathrm{i}\tilde{t}}} \int \mathrm{d}\zeta \ \exp\left[\mathrm{i}\theta_0 \varphi(\zeta,\tilde{z},\tilde{t})\right] \ , \tag{87}$$

with

$$\varphi(\zeta,\tilde{z},\tilde{t}) = \frac{(\tilde{z}-\zeta)^2}{2\tilde{t}} + \cos\zeta \ . \tag{88}$$

The relative density $|\psi(z,t)|^2$, initially unity, acquires spatial variations with the passage of time. For $\tilde{t} \ll 1$, relative density modulations are small. They grow linearly with $\tilde{t}$ and are oscillatory in $\tilde{z}$ with period 2π. Growth of density maxima with time culminates, for $\theta_0 \gg 1$, in the formation of caustics at times $\tilde{t} \gtrsim 1$. Caustics are determined by the vanishing of the first and second derivatives of the phase $\varphi(\zeta,\tilde{z},\tilde{t})$ with respect to ζ. The first requirement defines rays of atoms, while the second identifies the points at which the emerging rays are focused. The density at these points is found by computing the integral in Eq. (87), using the stationary phase method. Since the first two derivatives of $\varphi(\zeta,\tilde{z},\tilde{t})$ vanish, the integral is controlled by the third derivative, $\partial_\zeta^3 \varphi(\zeta,\tilde{z},\tilde{t})$, and has a value proportional to $\theta_0^{-1/3}$, resulting in a large relative density, $|\psi(\tilde{z},\tilde{t})|^2 \sim \theta_0^{1/3}$, with the characteristic for caustics aperiodic oscillations [94]. A numerical example is given in Fig. 5, where the relative density is plotted as a function of $\tilde{z}$ for three different values of $\tilde{t}$ (in this example $\theta_0 = 30$). Caustics are located at $\tilde{z} = 0$ for $\tilde{t} = 1$, and at $\tilde{z} \approx \pm 0.7$ for $\tilde{t} = 2$.

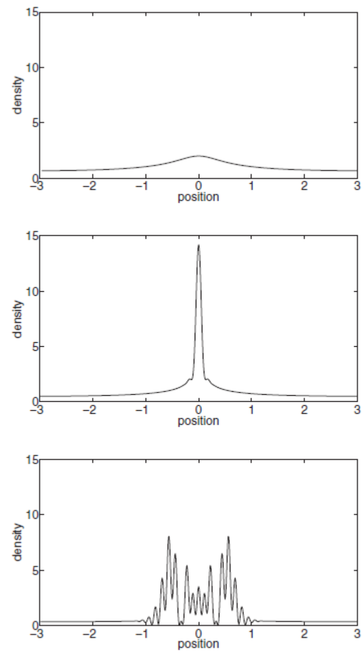

Figure 5: Relative density as a function of (dimensionless) position $\tilde{z}$, for $\theta_0 = 30$ and $\tilde{t} = 0.5$ (top), 1 (middle) and 2 (bottom). (Reprinted, with permission, from Phys. Rev. A **80** 013603 (2009)).

Eq. (86) for $\psi(z,t)$ applies also for a disordered potential and the mechanism for caustic formation is qualitatively the same as for the sinusoidal potential discussed above. Since the impressed phase $\theta(z')$ is now a random function, the formation of caustics is a matter of probability. The typical time for caustic formation is $t^* = mR_0^2/\hbar\theta_0$. Using the relations $\frac{1}{2}m\omega_\perp^2 a_\perp^2 = \mu$ and $\theta_0 = \pi V_0/2\hbar\omega_\perp$, the formation time can be written in terms of the experimentally controlled parameters as

$$t^* = \frac{4}{\pi\omega_\perp}\frac{\mu}{V_0}\left(\frac{R_0}{a_\perp}\right)^2 . \tag{89}$$

Quantitative analytic results for the second moment of the relative density, $\overline{|\psi(z,t)|^4} \equiv S(t) + 1$, can be found in [92]. The calculation is along the same lines as for the random screen problem in optics [95], where S is called the scintillation index and it is a measure of spatial intensity fluctuations

in the speckle pattern. For a uniform intensity S is clearly zero, and for the standard, fully developed speckle pattern S is unity. These two limits correspond, respectively, to short ($\tilde{t} << 1$) and long ($\tilde{t} >> 1$) times. In the more interesting intermediate time regime, when $\tilde{t} \gtrsim 1$, S is proportional to $\ln\theta_0 >> 1$, signalling the appearance at this time of caustics and the associated large density fluctuations.

Large density variations in an expanding condensate, released from a disordered trap, were observed in [17]. In this experiment $\mu/\hbar\omega_\perp = 5.6$, $R_0 = 15\mu$m, $a_\perp \sim 10\mu$m and the largest density variations were observed for $V_0 = 0.5\mu$, in a time of flight image at $t_{\rm ToF} = 8$ms, which is significantly larger than $1/\omega_\perp$, see Fig. 6(h).

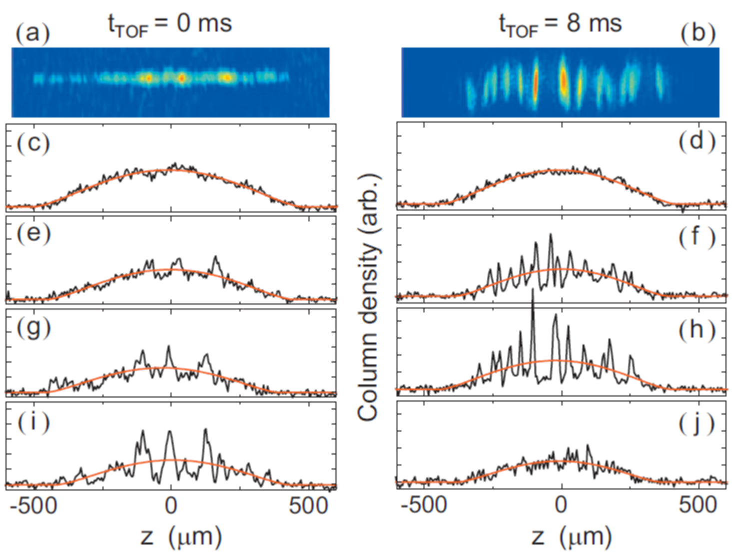

Figure 6: (c)-(j) *In situ* column density profiles on left and corresponding ToF profiles on right: (c),(d) $V_0 = 0$; (e),(f) $V_0 = 0.3\mu$; (g),(h) $V_0 = 0.5\mu$; and (i),(j) $V_0 = 1.0\mu$. Solid red lines are fits to Thomas-Fermi distributions. (Reprinted, with permission, from Phys. Rev. A **77**, 033632 (2008)).

The value $V_0 = 0.5\mu$ corresponds to a phase amplitude $\theta_0 = 4.4$ which gives the caustic formation time $t^* = 5$ms, comparable to the value of $t_{\rm ToF}$. While the value $\theta_0 = 4.4$ does not lie deep within the large θ_0 regime (the experiment was not designed for caustic observation), the large density variations in Fig. 6(h) can most likely be attributed to caustics. On the other

hand, a similar experiment performed in [93] cannot be interpreted in terms of caustics, as discussed in [92].

So far our discussion was limited to a strongly anisotropic, quasi-$1d$ BEC. Let us briefly comment on some other cases, referring the reader to [92] for details.

(i) $2d$ geometry. A quasi-$2d$ condensate is initially strongly confined in the axial z-direction (trap frequency ω_z), with only a weak confinement in the radial $\mathbf{r}_\perp$-direction. In addition, there is a random or a deterministic in-plane potential $V(\mathbf{r}_\perp)$. After all potentials are switched off and the condensate is freely expanding for a time $\sim 1/\omega_z$, it acquires a phase imprint $\theta(\mathbf{r}_\perp) \sim V(\mathbf{r}_\perp)/\hbar\omega_z$. At later times, in analogy with Eq. (86), the planar part of the condensate wave function is given by

$$\Phi(\mathbf{r}_\perp, t) = \frac{m}{2\pi \mathrm{i}\hbar t} \int \mathrm{d}^2\mathbf{r}'_\perp \exp\left[\frac{\mathrm{i}m}{2\hbar t}|\mathbf{r}_\perp - \mathbf{r}'_\perp|^2 + \mathrm{i}\theta(\mathbf{r}'_\perp)\right] . \tag{90}$$

As in quasi-one dimensional systems, caustics are formed for $\theta_0 \gg 1$ at values of the scaled time $\tilde{t} \sim 1$, and in this regime Eq. (90) can be evaluated using the stationary phase method. Unlike the quasi-$1d$ case, now caustics form a set of lines rather than a set of isolated points. The theory of caustic formation resulting from a random phase $\theta(\mathbf{r}_\perp)$ is analogous to the treatment of the phase screen problem, which has been studied extensively for two-dimensional systems in the context of optics [94]. In particular, the morphology of caustic lines for the random case is discussed in [96].

(ii) interacting bosons in $1d$. Here the transverse confinement is very tight: $\hbar\omega_\perp$ is much larger than the characteristic interaction energy so that, with respect to transverse motion, all N atoms in the trap reside in the ground state $\chi_0(\rho)$ of the harmonic oscillator, forming a strictly one-dimensional system. The axial motion is controlled by an effective one-dimensional Hamiltonian – the Lieb-Liniger model [97, 98]. At some instance the radial confinement is switched off and, simultaneously, a short potential pulse is applied to the system, creating a prescribed phase imprint $\theta(z)$ which can be a deterministic or a random function of z. It has a characteristic amplitude θ_0 and scale of variation R_0. The system is beyond mean field theory and the whole many-body wave function has to be considered. Initially, i.e. just after switching off the trap and making the phase imprint, the axial part of the

many-body function is

$$\Psi(z_1, \ldots z_N; t{=}0) = \exp\left[\mathrm{i}\sum_{j=1}^{N}\theta(z_j)\right]\Phi_0(z_1, \ldots z_N) \tag{91}$$

where $\Phi_0(z_1, \ldots z_N)$ is the ground state wavefunction, prior to the action of the pulse. In the course of expansion, large density variations can develop, including formation of caustics. One must, however, account for the momentum distribution function $n(p)$ of the system of interacting bosons (in the mean field approach $n(p) = 2\pi\delta(p)$). It is clear that a broad momentum distribution will impede focusing of the atomic rays and, thus, formation of caustics. The width of the distribution $n(p)$ depends on the strength of interactions and, roughly, it is determined by the inverse coherence length $1/\xi_c$. It is shown in [92] that the necessary condition for caustics is $\xi_c n_1 \gg 1$, where n_1 is the one-dimensional density. This condition can be satisfied only in the weak interaction limit. In the opposite limit of strong interactions (hard core bosons) $\xi_c \approx 1/n_1$ and the caustics are suppressed.

(iii) 1d *Fermi gas.* Similarly to bosons, one can consider the dynamics of fermions, with an initially impressed phase that varies periodically or randomly as a function of position z. For a 1d Fermi gas the problem is similar to that of the previous item. The particle statistics manifests itself only through the momentum distribution of particles before the expansion, and the Fermi wavelength λ_{F} is taking the place of the coherence length ξ_c of the Lieb-Liniger gas. Since $\lambda_{\mathrm{F}} n_1 \sim 1$, caustics are absent from the Fermi gas, for the same reason as in the Bose gas with hard-core interactions. The main difference between non-interacting fermions and hard-core bosons stems from the Fermi surface discontinuity in the momentum distribution. Within the approximations of geometrical optics, this discontinuity leads to sharp peaks in the derivative of the density (with respect to position z or time t), rather than in the density itself.

7 Conclusions

Several topics concerning the behavior of cold atomic gases in the presence of disorder have been reviewed. This is a relatively new and rapidly progressing subject which poses some questions, not previously encountered in condensed matter physics. One such question pertains to Anderson localization in a 3d speckle potential, with its rather unusual anisotropic, long-range

correlations. It is not yet clear how these peculiarities affect the standard picture of Anderson localization and work in this direction has just begun [10, 11, 49]. Even such basic quantity as the average density of states is not well known for this kind of a random potential and the problem awaits careful theoretical investigation.

In the experimental setup of [10, 11] one observes the time evolution of an atomic cloud (BEC or fermions) in the presence of a random potential. In the long time limit, part of the cloud diffuses away and the rest remains localized. To obtain an accurate value for the localization length and for the exponent ν one has to measure the long tail of the localized part (or the very slowly diffusing part, originating form the energy components close to E_c). So far such measurements are beyond reach. Another possibility, mentioned in [11], would be to prepare a collection of atoms with a narrow energy distribution and to study its evolution in a random potential. This would allow to "isolate" the transition region from the rest of the spectrum.

One of the most challenging problems in condensed matter physics is the combined effect of interactions and disorder. Since non-interacting bosons correspond to to a singular, pathological limit, it is clear that the interactions must be accounted for from the start. Already the Gross-Pitaevskii mean field theory for disordered bosons leads to the interesting and difficult problem of the $2d$ and $3d$ non-linear Schrödinger equation with a random potential. Two of the recently addressed theoretical problems in this context are the time evolution of a "matter wave packet" [74, 75, 76] and the flow of a BEC through a disordered region [99]. Things get more involved when one tries to go beyond mean field. Even the nature of the ground state, and the zero-temperature superfluid-insulator transition, is only qualitatively understood [39, 40]. Finite temperature introduces a further dimension to the problem and allows for a number of phase transitions. In particular, it has been argued [64] that in $2d$ no direct superfluid-insulator transition is possible at finite temperature and that, under increase of disorder, the system of weakly interacting bosons must pass through a normal fluid state. (In $3d$ the sharp fluid-insulator transition is replaced by a crossover). The combined effect of interactions, disorder and temperature (beyond the scope of this review) will surely receive much attention in the future.

8 Acknowledgments

I am indebted to L. Beilin, J. Chalker, E. Gurevich, P. Henseler, A. Minguzzi, S. Skipetrov and B. van Tiggelen for collaboration on some of the topics presented in this review. I am grateful to J. Chalker, E. Gurevich, S. Lipson, C. Müller, D. Polyakov, M. Raikh, M. Segev and S. Skipetrov for extensive discussions and correspondence which led to clarification of a number of specific topics addressed in this review. Useful conversations and correspondence with I. Aleiner, B. Altshuler, A. Aspect, N. Cherroret, J. Feinberg, A. Genack, F. Jendrzejewski, S. Kondov, B. DeMarco, C. Miniatura, M. Piraud and L. Sanchez-Palencia are gratefully acknowledged.

References

[1] Aspect A and Inguscio M 2009 Phys. Today **62** 30

[2] Sanchez-Palencia L and Lewenstein M 2010 Nature Phys. **6**, 87

[3] Fallani L, Fort C and Inguscio M 2008 *Advances in Atomic, Molecular and Optical Physics* **56** 119

[4] Modugno G 2010 Rep. Prog. Phys. **73** 102401

[5] Lewenstein M, Sanpera A, Ahufinger V, Damski B, Sen (De) A, and Sen U 2007 Adv. Phys. **56** 243

[6] Müller C A and Delande D 2009 *Ultracold Gases and Quantum Information*, Les Houches XCI, p.441

[7] Billy J, Josse V, Zuo Z, Bernard A, Hambrecht B, Lugan P, Clément D, Sanchez-Palencia L, Bouyer P and Aspect A 2008 *Nature* **453** 891

[8] Roati G, D'Errico C, Fallani L, Fattori M, Fort C, Zaccanti M, Modugno G, Modugno M and Inguscio M 2008 *Nature* **453** 895

[9] Robert-de-Saint-Vincent M, Brantut J.-P., Allard B, Plisson T, Pezzé L, Sanchez-Palencia L, Aspect A, Bourdel T, and Bouyer P 2010 Phys. Rev. Lett. **104** 220602

[10] Kondov S S, McGehee W R, Zirbel J J, and DeMarco B 2011 Science **334** 66

[11] Jendrzejewski F, Bernard A, Müller K, Cheinet P, Josse V, Piraud M, Pezzé L, Sanchez-Palencia L, Aspect A, and Bouyer P 2011 arXiv:1108.0137

[12] Pitaevskii L and Stringari S 2003 *Bose-Einstein Condensation*, Clarendon Press

[13] Pethick C J and Smith H 2002 *Bose-Einstein Condensation in Dilute Gases*, Cambridge University Press

[14] Clément D, Varon A F, Hugbart M, Retter J A, Bouyer P, Sanchez-Palencia L, Gangardt D M, Shlyapnikov G V, and Aspect A 2005 Phys. Rev. Lett. **95** 170409

[15] Clément D, Varon A F, Retter J A, Sanchez-Palencia L, Aspect A, and Bouyer P 2006 New. J. Phys. **8** 165

[16] Fort C, Fallani L, Guarrera V, Lye J E, Modugno M, Wiersma D S, and Inguscio M 2005 Phys. Rev. Lett. **95**, 170410

[17] Chen Y P, Hitchcock J, Dries D, Junker M, Welford C, and Hulet R G 2008 Phys. Rev. A **77** 033632

[18] Goodman J W 2007 Speckle Phenomena in Optics, Roberts and Company, Englewood, Colorado

[19] Giglio M, Carpineti M and Vailati A 2000 Phys. Rev. Lett. **85** 1416

[20] Cerbino R 2007 Phys. Rev. A **75** 053815

[21] Gatti A, Magatti D and Ferri F 2008 Phys. Rev. A **78** 063806

[22] Magatti D, Gatti A and Ferri F 2009 Phys. Rev. A **79** 053831

[23] Lipson A, Lipson S G and Lipson H S 2010 *Optical Physics*, Cambridge

[24] Goodman J W 2005 Introduction to Fourier Optics, Roberts and Company, Englewwod, Colorado

[25] see Eq. (17) in [22], with $z_1 \equiv z$ and with the ratio z_1/z_2 in the exponent set equal to unity.

[26] Kuhn R C, Sigwarth O, Miniatura C, Delande D and Müller C A 2007 New Jour. Phys. **9** 161

[27] Miniatura C, Kuhn R C, Delande D, and Müller C A 2009 Eur. Phys. J. B **68** 353

[28] Pezzé L, Robert-de-Saint-Vincent M, Bourdel T, Brantut J.-P., Allard B, Plisson T, Aspect A, Bouyer P, and Sanchez-Palencia L 2011 New Jour. Phys. **13** 095015

[29] Gavish U and Castin Y 2005 Phys. Rev. Lett. **95** 020401

[30] Gadway B, Pertot D, Reeves J, Vogt M, Schneble D 2011 Phys. Rev. Lett. **107** 145306

[31] Shklovskii B I and Efros A L 1984 *Electronic Properties of Doped Semiconductors* , Springer

[32] Lifshits I M, Gredeskul S A and Pastur L A 1988 *Introduction to the Theory of Disordered Systems*, Wiley

[33] Lee P A and Ramakrishnan T V 1985 Rev. Mod. Phys. **57** 287

[34] Kramer B and MacKinnon A 1993 Rep. Prog. Phys. **56** 1469

[35] E. Akkermans and G. Montambaux 2007 *Mesoscopic Physics of Electrons and Photons*, Cambridge University Press

[36] Efetov K 1997 *Supersymmetry in Disorder and Chaos*, Cambridge

[37] Mirlin A D 2000 Phys. Rep **326** 259

[38] Vollhardt D and Wölfle p 1992 in *Electronic phase transitions* Eds. W. Hanke and Y. V. Kopaev (Elsevier, Amsterdam)

[39] Shklovskii B I 2008 Semiconductors (St. Petersburg) **42** 927

[40] Falco G M, Natterman T and Pokrovsky V L, 2009 Phys. Rev. B **80** 104515

[41] Anderson P W 1958 Phys. Rev. **109** 1492

[42] Landau L D and Lifshitz E M 1997 Quantum Mechanics (Third Edition), Butterworth - Heinemann.

[43] Slevin K and Ohtsuki T 1999 Phys. Rev. Lett. **82** 382

[44] Skipetrov S E, Minguzzi A, van Tiggelen B A and Shapiro B 2008 Phys. Rev. Lett. **100** 165301

[45] Yedjour A and Van Tiggelen B A 2010 Eur. Phys. J. D **59** 249

[46] Halperin B I and Lax M 1966 Phys. Rev. **148** 722

[47] Zittartz J and Langer J S 1966 Phys. Rev. **148** 741

[48] Falco G M, Fedorenko A A, Giacomelli J and Modugno M 2010 Phys. Rev. A **82** 053405

[49] Piraud M, Pezzé L and Sanchez-Palencia L 2011 arXiv:1112.2859

[50] M. I. Dyakonov and A. V. Khaetskii 1991 Sov. Phys. JETF **72** 590

[51] The diffusion coefficient here should be inderstood as averaged over various initial positions of the diffusing particle.

[52] Zallen R 1983 *The Physics of Amorphous Solids*, Wiley & Sons

[53] Shapiro B 1983 "Localization versus percolation", in *Percolation Structures and Processes*, p. 367, Eds. G. Deutscher, R. Zallen and J. Adler (Bristol: Adam Hilger)

[54] Pilati S, Giorgini S, Modugno M, and Prokof'ev N 2010 New J. Phys. **12** 073003

[55] Abrahams E, Anderson P W, Licciardello D C and Ramakrishnan T V 1979 Phys. Rev. Lett. **42** 673

[56] Apalkov V M, Raikh M E and Shapiro B 2003 in *"Anderson Localization and its Ramifications"* Springer, 'Lecture Notes in Physics', ed. T. Brandes and S. Kettermann, p. 119

[57] Shapiro B 2007 Phys. Rev. Lett. **99**, 060602

[58] Pollak M and Ortuno M 1985 *Electron-electron interactions in disordered systems* eds. Efros A L and Pollak M, North-Holland, 287

[59] Reppy J D 1992 J. Low Temp. Phys. **87** 205

[60] Pasienski M, McKay D, White M and DeMarco B 2010 Nature Physics **6** 667

[61] Deissler B, Zaccanti M, Roati G, D'Errico C, Fattori M, Modugno M, Modugno G, and Ignuscio M 2010 Nature Physics **6** 354

[62] Gaul C and Müller C A 2011 Phys. Rev. A **83** 063629

[63] Lugan P and Sanchez-Palencia L 2011 Phys. Rev. A **84** 013612

[64] Aleiner I L, Altshuler B L and Shlyapnikov G V 2010 Nature Physics **6** 900

[65] Huang K and Meng H-F 1992 Phys. Rev. Lett. **69**644

[66] Giorgini S, Pitaevskii L and Stringari S 1994 Phys. Rev. B **49**12938

[67] Lee D K K and Gunn J M F 1990 J. Phys. Cond. Matter **2** 7753

[68] Kagan Yu, Surkov E L and Shlyapnikov G V 1996 Phys. Rev. A**54** R1753

[69] Castin Y and Dum R 1996 Phys. Rev. Lett. **77** 5315

[70] Sanchez-Palencia L, Clément D, Lugan P, Bouyer P, Shlyapnikov G V, and Aspect A 2007 Phys. Rev. Lett. **98** 210401

[71] Chalker J T 1990 Physica A **167** 253

[72] Henseler P and Shapiro B 2008 Phys.Rev. A **77** 033624

[73] Cherroret N and Skipetrov S E 2008 Phys. Rev. Lett. **101** 190406

[74] Cherroret N and Skipetrov S E 2009 Phys. Rev. A **79** 063604

[75] Schwiete G and Finkel'stein A M 2010 Phys. Rev. Lett. **104** 103904

[76] Cherroret N and Wellens T 2011 Phys. Rev. A **84** 021114

[77] Wegner F 1976 Z. Phys. B**25** 327

[78] Fishman S, Grempel D R and Prange R E 1982 Phys. Rev. Lett. **49** 509

[79] Moore F L, Robinson J C, Bharucha C F, Sundaram B and Raizen M G 1995 Phys. Rev. Lett. **75** 4598

[80] Casati G, Guarneri I and Shepelyansky D L 1989 Phys. Rev. Lett. **62** 345

[81] Chabé J, Lemarié G, Grémaud B, Delande D, Szriftgiser P and Garreau J-C 2008 Phys. Rev. Lett. **101** 255702

[82] Lemarié G, Chabé J, Szriftgiser P, Garreau J-C, Grémaud B and Delande D 2009 Phys. Rev. A **80** 043626

[83] Lopez M, Clément J-F, Szriftgiser P, Garreau J-C and Delande D 2011 arXiv:1108.0630

[84] Giorgini S, Pitaevskii L P and Stringari S 2008 Rev. Mod. Phys. **80** 1215

[85] Y. Castin, in "Ultra-cold Fermi gases", Proc. Inter. School of Physics "Enrico Fermi", Varenna, Eds. M. Inguscio, W. Ketterle and C. Salomon, p.289 (2007).

[86] Beilin L, Gurevich E and Shapiro B 2010 Phys. Rev. A **81** 033612

[87] In the mean field Gross-Pitaevskii theory, with its "classical" macroscopic wave function, the quantum average is implicit and only averaging over the realization of disorder remains.

[88] Leggett A J 2001 Rev. Mod. Phys. **73** 307

[89] Altman E, Demler E and Lukin M D 2004 Phys. Rev. A **70**, 013603

[90] Landau L D and Lifshitz E M 1980 Statistical Physics, part 1, Butterworth- Heinemann

[91] Nagornykh P and Galitski V 2007 Phys. Rev. A **75** 065601

[92] Chalker J T and Shapiro B 2009 Phys. Rev. A **80** 013603

[93] Clément D, Bouyer P, Aspect A, and Sanchez-Palencia L 2008 Phys. Rev. A **77** 033631

[94] Berry M V 1977 J. Phys. A **10** 2061

————-1976 Adv. Phys. **25** 1

[95] Jakeman E and McWhirter J G 1977 J. Phys. A **10** 1599

[96] Berry M V, 1980 Proc. Symp. App. Maths **36** 13.

[97] Lieb E H and Liniger W 1963 Phys. Rev. **130** 1605

[98] Olshanii M 1998 Phys. Rev. Lett. **81** 938

[99] Paul T, Albert M, Schlagheck P, Leboeuf P and Pavloff N 2009 Phys. Rev. A **80** 033615